Vascular Function in Chronic Renal Failure

Lisa Nguy

Department of Molecular and Clinical Medicine
Institute of Medicine
Sahlgrenska Academy, University of Gothenburg

UNIVERSITY OF GOTHENBURG

Gothenburg 2014

Cover illustration: Important notes by Lisa Nguy

Vascular Function in Chronic Renal Failure

lisa.nguy@gu.se

ISBN 978-91-628-8886-2

Printed in Gothenburg, Sweden 2014
Tryckeri Kompendiet

“ Let us read, and let us dance;
these two amusements will never do any harm to the world.”

– Voltaire

Vascular Function in Chronic Renal Failure

Lisa Nguy
Department of Molecular and Clinical Medicine,
Institute of Medicine at Sahlgrenska Academy, University of Gothenburg
Göteborg, Sweden

ABSTRACT

A majority of patients with chronic kidney disease (CKD) die of cardiovascular (CV) disease before reaching end-stage renal disease. The causes of CV death in CKD are characterized by an excess of sudden cardiac deaths compared to the general population. Arterial defects that are typical in these patients are aortic stiffness and media calcifications. Maladaptive changes in vascular smooth muscle cells (VSMCs) take place in response to mineral metabolism disorders that develop with declining kidney function. The aims of the present studies were: 1) to investigate the effects of chronic renal failure (CRF) on resistance arteries and aorta in rats with adenine-induced CRF (A-CRF); 2) to determine by which mechanisms A-CRF rats develop hypertension and to investigate whether reduced aortic relaxation rate is associated with increased aortic stiffness; 3) to investigate the presence of reduced relaxation rate in other conduit arteries and to elucidate underlying mechanisms of this vascular defect through gene expression analyses; and 4) to investigate the effects of a high NaCl intake on arterial functions and aortic relaxation rate in A-CRF rats. We found that rats with A-CRF develop a reduced rate of relaxation, mainly in the thoracic aorta, but also in other major conduit arteries. This was associated with an increased aortic stiffness and was independent of vascular calcification. A-CRF rats developed salt-sensitive and renin-independent hypertension. High NaCl intake impaired relaxation in aortic VSMCs and augmented the reduction in aortic relaxation rate. Significantly altered expressions of several genes that are critically involved in excitation-contraction coupling of aortic VSMCs were found. Our findings provide a possible link between CRF and the development of aortic stiffness, which in the future may unravel novel therapeutic targets. Such therapies have the potential to improve life expectancy in patients with CKD.

Keywords: cardiovascular, chronic renal failure, hypertension

ISBN: 978-91-628-8886-2

SAMMANFATTNING PÅ SVENSKA

Majoriteten av patienter med kronisk njursvikt dör av hjärt-kärlsjukdomar. Dialysbehandlade patienter har en kraftigt ökad risk för kardiovaskulär död jämfört med åldersmatchade friska. Artärförändringar vid nedsatt njurfunktion karaktäriseras av ökad artärstelhet och förkalkningar av kärlväggen. Aortastelhet är en kraftfull oberoende riskfaktor för död. Mekanismerna som orsakar artärförändringarna är i stort okända och därför har målet med denna avhandling varit att utreda dessa i syfte att finna nya behandlingar.

För att i detalj och under standardiserade förhållanden kunna studera dessa mekanismer har vi använt oss av en djurexperimentell modell av kronisk njursvikt; nämligen adenin-orsakad njursvikt på råtta.

Hos råttor med kronisk njursvikt fann vi att thorakalaorta, tillsammans med andra stora kärl, hade en förlångsammad relaxationshastighet. Den långsammare relaxationen av aorta var associerad med en ökad aortastelhet som utvecklades i frånvaro av förkalkningar. Utöver detta utvecklade råttorna i vår njursviktmodell högt blodtryck, som visade sig vara oberoende av renin, ett enzym som normalt frisätts för att höja blodtryck. Vi testade effekterna av ett högt saltintag och fann att det redan höga blodtrycket höjdes ytterligare, samt att den förlångsammade relaxationshastigheten i aorta blev än mer uttalad. Funktionella studier avslöjade att glatta muskellceller i aorta hade en nedsatt förmåga att relaxera. Vi kartlade genuttrycket i thorakalaorta och fann skillnader mellan kontrollråttor och njursviktande råttor i gener som är involverade i regleringen av intracellulära nivåer av kalcium i glatta muskelceller. Avvikelserna i genuttryck hos de njursviktande råttorna var förenliga med ökade koncentrationer av kalcium i cytoplasman i glatta muskelceller och ökad kärltonus.

Sammanfattningsvis har vi funnit nya samband mellan kronisk njursvikt och aortas funktion och då särskilt relaxationsförmågan och kärlstelhet. Genom att kartlägga de underliggande mekanismerna hoppas vi i framtiden kunna utveckla nya behandlingar mot kärlstelhet och därmed förbättra prognosen för kroniskt njursviktande patienter som löper en kraftigt ökad risk för kardiovaskulär sjukdom och död.

LIST OF PUBLICATIONS

This thesis is based on the following studies, referred to in the text by their Roman numerals.

I. Vascular function in rats with adenine-induced chronic renal failure
Nguy L, Nilsson H, Lundgren J, Johansson ME, Teerlink T, Scheffer PG, Guron G.

Am J Physiol Regul Integr Comp Physiol. 2012 Jun 15;302(12):R1426-35.

II. Rats with adenine-induced chronic renal failure develop low-renin, salt-sensitive hypertension and increased aortic stiffness
Nguy L, Johansson ME, Grimberg E, Lundgren J, Teerlink T, Carlström M, Lundberg JO, Nilsson H, Guron G.

Am J Physiol Regul Integr Comp Physiol. 2013 May 1;304(9):R744-52.

III. Adenine-induced chronic renal failure causes decreased aortic relaxation rate and altered expression of genes involved in excitation-contraction coupling in vascular smooth muscle cells
Nguy L, Shubbar E, Jernås M, Nookaew I, Lundgren J, Olsson B, Nilsson H, Guron G.

In manuscript

IV. High NaCl intake aggravates aortic dysfunction in rats with adenine-induced chronic renal failure
Nguy L, Shubbar E, Nilsson H, Guron G.

In manuscript

TABLE OF CONTENTS

ABBREVIATIONS

8-OHdG	8-hydroxy-2-deoxyguanosine
ACh	acetylcholine
A-CRF	adenine-induced chronic renal failure
ADMA	asymmetric dimethylarginine
AI	augmentation index
Ang II	angiotensin II
AP	arterial pressure
BW	body weight
Casq	calsequestrin
C_{Cr}	creatinine clearance
CKD	chronic kidney disease
COX	cyclooxygenase
CPI-17	C-kinase potentiated protein phosphatase-1 inhibitor 17 kDa
CRAC	calcium release-activated channel
CRF	chronic renal failure
CSF	cerebrospinal fluid
CV	cardiovascular
d_{100}	internal diameter at 100 mmHg
DHA	2,8-dihydroxyadenine
EDCF	endothelium-derived contracting factor
EDHF	endothelium-derived hyperpolarizing factor
EDRF	endothelium-derived relaxing factor
EO	endogenous ouabain
ESRD	end-stage renal disease
GFR	glomerular filtration rate
GPCR	G-protein-coupled receptor
HPLC	high-performance liquid chromatography
HR	heart rate
IP_3	inositol 1,4,5-triphosphate
L-Arg	L-arginine
L-NAME	Nω-nitro-L arginine-methyl ester hydrochloride

LVEDP	left ventricular end-diastolic pressure
LVH	left ventricular hypertrophy
MAP	mean arterial pressure
MDA	malondialdehyde
RLC	myosin regulatory light chain
MLCK	myosin light-chain kinase
MLCP	myosin light-chain phosphatase
NCX	Na/Ca-exchanger
NE	norepinephrine
NKA	Na,K-ATPase
NO	nitric oxide
NOS	nitric oxide synthase
PE	phenylephrine
Pln	phospholamban
PRA	plasma renin activity
PSS	physiological salt solution
PTH	parathyroid hormone
PWV	pulse wave velocity
qRT-PCR	quantitative real-time polymerase chain reaction
RAS	renin-angiotensin system
ROCK	Rho-kinase
SBP	systolic blood pressure
SDMA	symmetric dimethylarginine
SERCA	sarcoendoplasmic reticulum calcium ATPase
SHR	spontaneously hypertensive rats
SNP	sodium nitroprusside
SR	sarcoplasmic reticulum
Stim1	stromal interaction molecule 1
Trpc4	transient receptor potential cation channel 4
VGCC	voltage-gated calcium channel
VSM	vascular smooth muscle
VSMC	vascular smooth muscle cell
WKY	Wistar Kyoto rats

1 INTRODUCTION

Patients with chronic kidney disease (CKD) face substantial reduction in life expectancy, mainly contributed by cardiovascular (CV) disease, compared to individuals with normal renal function.[1] The majority of CKD patients die from CV disease even before reaching end-stage renal disease (ESRD),[2] the stage at which dialysis or kidney transplantation are essential for survival. There is a high prevalence of traditional CV risk factors in CKD, such as diabetes, hypertension, hypercholesterolemia and atherosclerosis.[3] These risk factors are not entirely responsible for the increased CV risk, as studies on children and young adults with CKD without comorbidities reveal that the CV risk is still markedly increased compared to the age-matched general population.[4]

This thesis focuses mainly on the vascular dysfunctions in chronic renal failure (CRF), in an attempt to elucidate the mechanisms underlying the increased CV risk, without the confounding effects of comorbidities.

1.1 The kidney

To properly understand the impact of renal insufficiency on the circulatory system, an overview of renal and vascular physiology is necessary.

The kidney plays a key role in the CV system as its major functions are to maintain the composition and volume of body fluids, thereby maintaining arterial pressure (AP), regulate excretion of electrolytes and water, maintain acid-base balance, maintain mineral metabolism, and to stimulate red blood cell (erythrocyte) production by producing and secreting erythropoietin.

1.1.1 Renal blood pressure regulation

The kidney controls AP through multiple mechanisms, including the renin-angiotensin system (RAS). When AP decreases this is sensed by juxtaglomerular cells in afferent renal arterioles, resulting in the release of the enzyme renin. Renin acts on angiotensinogen to form angiotensin I, which is further cleaved into angiotensin II (Ang II) by angiotensin converting enzyme.[5] Ang II, a powerful vasoconstrictor, raises AP by increasing total

peripheral resistance and stimulates secretion of aldosterone from the adrenal glands, which in turn stimulates sodium and water reabsorption, and potassium secretion, in the kidney.[5] Furthermore, Ang II increases thirst and triggers release of antidiuretic hormone,[6] causing water reabsorption in collecting ducts.

The kidney also regulates AP through the pressure-natriuresis mechanism. Increased AP results in increased urinary sodium excretion which will reduce AP by decreasing extracellular fluid volume.

1.2 Sympathetic control of blood pressure

The sympathetic nervous system innervates small arteries and arterioles in almost all tissues, but also the renal tubules and the juxtaglomerular cells.[5] Increased renal sympathetic nerve activity will stimulate renin release, directly increase renal tubular sodium reabsorption, and constrict the renal arterial vasculature.[7]

Renal sympathetic nerve activity is influenced by baroreceptors. These are stretch receptors that are mostly abundant in the wall of the aortic arch and the carotid sinus, although also present in the cardio-pulmonary system. Baroreceptors are responsible for the rapid control of changes in AP. An increase in AP causes stretching of the arterial wall, resulting in increased signaling of the baroreceptors to the brain. Outgoing signals from the brain then decrease signaling through the sympathetic vasoconstrictor fibers, and increase parasympathetic signaling to the heart, which leads to vasodilatation of the peripheral vasculature and a decreased heart rate (HR).[5] On the contrary, decreased AP causes increased sympathetic activity and decreased parasympathetic signaling, leading to peripheral vasoconstriction, increased HR, and elevated AP.

1.3 The circulatory system

The arterial wall consists of three components: tunica adventitia, tunica media, and tunica intima. The adventitia is the outermost layer of the vessel and consists of connective tissue made up of elastin and collagen, fibroblasts, mast cells, macrophages and nerve axons.[8-9] Tunica media is composed of

layers of vascular smooth muscle cells (VSMCs) that are circumferentially arranged, and are in some arteries separated from the adventitia by an external elastic lamina.[9] The thickness of the adventitia and media vary among different types of vessels. Single-layer endothelial cells, longitudinally arranged along the vessel, are supported by the internal elastic lamina on the luminal side of the media; this tunica intima is in direct contact with the blood.

Vascular smooth muscle cells

The sympathetic vasoconstrictor fibers are in contact with the outermost VSMCs of the media, where they release norepineprine (NE) for the elicitation of muscle contraction.[10] The intracellular mechanisms of vascular smooth muscle (VSM) excitation-contraction coupling are described and illustrated below (Figure 1).

It is the rise and fall in intracellular free calcium concentration that are mainly responsible for muscle contraction and relaxation, respectively.[11] When the intracellular calcium level increases, it binds to calmodulin, forming a complex with the catalytic subunit of myosin light-chain kinase (MLCK) and thereby activates this enzyme for the phosphorylation of the myosin regulatory light chain (RLC).[12] The myosin ATPase head becomes active, attaches to actin filaments and enables contraction.[13] A fall in calcium levels inactivates MLCK, and permits dephosphorylation of the RLC via myosin light-chain phosphatase (MLCP), resulting in relaxation.[14] Thus, it is the ratio between the activities of MLCK and MLCP that determines the level of contraction.

Increase in intracellular calcium levels is caused mainly by influx from the extracellular fluid, but also by release from intracellular stores. Activation of smooth muscle occurs through two mechanisms, pharmacomechanical coupling and electromechanical coupling.[15] The first-mentioned involves G-protein-coupled receptor (GPCR) activation. When, for example, NE interacts with α-adrenergic receptors, this facilitates an intracellular signaling cascade that leads to production of inositol 1,4,5-triphosphate (IP_3). IP_3 triggers release of calcium from the sarcoplasmic reticulum (SR) through activation of calcium release channels, IP_3 receptors (IP_3R).[16] The IP_3R-mediated calcium release triggers calcium release through ryanodine receptors also.[17] This is known as calcium-induced calcium release. In addition to this, GPCR signaling modulates the calcium sensitivity of myosin

by inhibiting MLCP via activation of C-kinase potentiated protein phosphatase-1 inhibitor 17 kDa (CPI-17),[18] through protein kinase C, and the RhoA-associated Rho-kinase (ROCK) pathway. The latter results in inactivation of MLCP either directly by ROCK, or through phosphorylation of CPI-17 by ROCK.[19] Electromechanical coupling refers to VSMC activation initiated by changes in membrane potential, e.g, depolarization. During such an event, the membrane potential increases, opens voltage-gated calcium channels (VGCC) for extracellular calcium influx and activates ryanodine receptors, all of which triggers contraction.[20-21]

During VSMC relaxation, calcium-activated potassium channels hyperpolarize the plasma membrane,[22] VGCC close, and intracellular calcium stores are restored by the sarcoendoplasmic reticulum calcium ATPase (SERCA). Extrusion of calcium is facilitated by the plasma membrane calcium ATPase (PMCA), and the Na/Ca-exchanger (NCX).[23] NCX is driven by the electrochemical gradient of sodium, which is maintained by the Na,K-ATPase (NKA).

Endothelial cells

The fact that the endothelium can regulate VSM tone was recognized in 1980, when Furchgott and Zawadzki reported that acetylcholine (ACh) caused endothelium-dependent relaxation of rabbit aorta.[24] The relaxation was caused by an endothelial-derived relaxing factor (EDRF), which later was found to be nitric oxide (NO). As shown in Figure 1, activation (by ACh) of muscarinic receptors on endothelial cells triggers store-released calcium, and activates endothelial NO synthase (NOS) for the production of NO. Activation of NOS is also triggered by increased shear stress of blood flow.[25] Prostacyclin (PGI_2), a product of the cyclooxygenase (COX) pathway, has also been identified as an EDRF. EDRFs that are not blocked by inhibition of NOS and COX are referred to as endothelial-derived hyperpolarizing factors (EDHFs). Apart from EDRFs and EDHFs there are also endothelial-derived contracting factors (EDCFs), which causes VSM contraction. The mechanisms of EDHFs and EDCFs will not be discussed in this thesis.

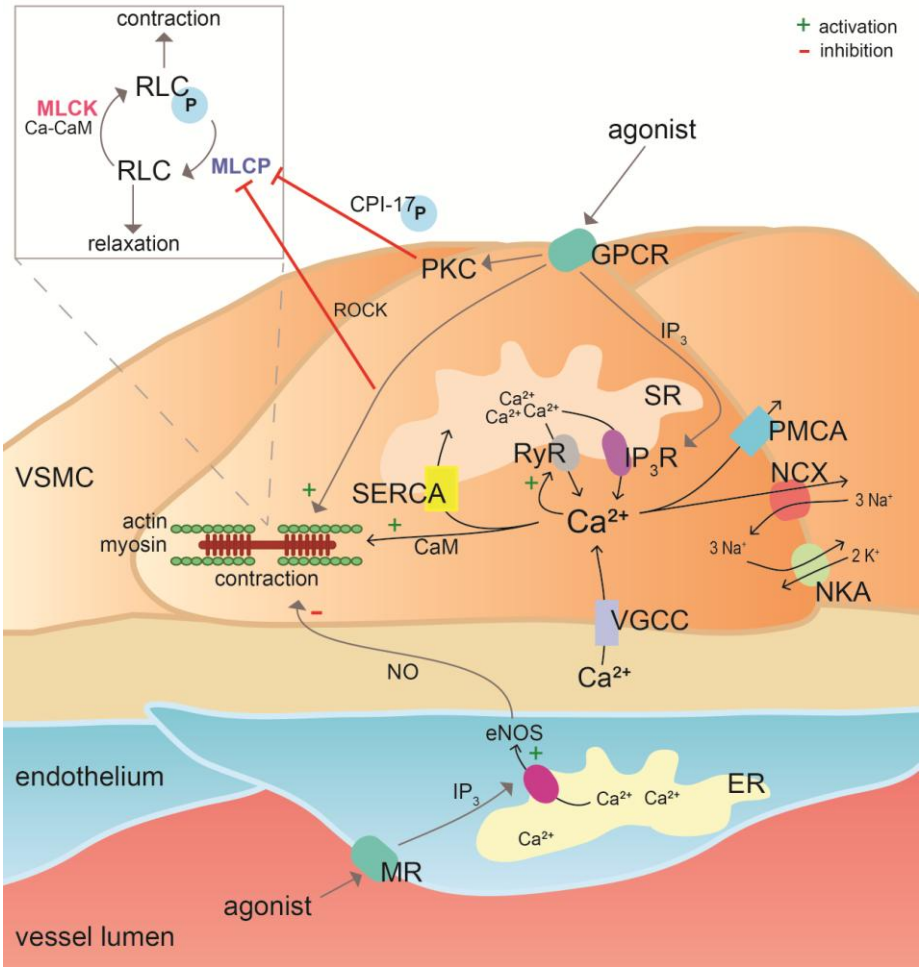

Figure 1. Intracellular mechanisms of excitation-contraction coupling in a vascular smooth muscle cell (VSMC). CaM, calmodulin; Ca-CaM, calcium-calmodulin; CPI-17, C-kinase potentiated protein phosphatase-1 inhibitor 17 kDa; GPCR, G-protein-coupled receptor; ER, endoplasmic reticulum; IP_3, inositol 1,4,5-triphosphate; IP_3R, IP_3 receptor; RLC, myosin regulatory light chain; MLCK, myosin light-chain kinase; MLCP, myosin light-chain phosphatase; MR, muscarinic receptor; NCX, Na/Ca-exchanger; NE, norepinephrine; NKA, Na,K-ATPase; NO, nitric oxide; NOS, nitric oxide synthase; PKC, protein kinase C; PMCA, plasma membrane calcium ATPase; ROCK, Rho-kinase; RyR, ryanodine receptor; SERCA, sarcoendoplasmic reticulum calcium ATPase; SR, sarcoplasmic reticulum; VGCC, voltage-gated calcium channel.

1.4 Chronic renal failure

Chronic renal failure (CRF) is most often the result of a gradual decline in kidney function over time and the stage at which the kidneys are no longer able to adequately filter blood and maintain homeostasis. Chronic kidney disease (CKD) includes conditions that cause structural or functional abnormalities of the kidney for a duration of at least 3 months, with or without decreased glomerular filtration rate (GFR).[26] GFR is the flow rate at which fluid is filtered across glomerular capillary walls of the nephrons, which are the basic structural and functional units of the kidney.

1.4.1 Cardiovascular mortality in CKD

Many epidemiological studies have established the association between CKD and CV disease.[27-31] Life expectancy is substantially reduced in patients with impaired kidney function,[1, 32] and a majority of them die of CV events before reaching ESRD. Mortality rates of patients undergoing dialysis treatment are at least 10- to 20-fold higher compared to the general population.[3] The CV risk is already increased when GFR falls below 60 ml/min per 1.73 m^2,[27] which is approximately 50% of normal GFR, and the risk of CV mortality is much higher than the risk of developing ESRD.[28, 33] Compared to the general population, the causes of CV death are different in patients with CKD, with a high prevalence of sudden cardiac deaths.[3] Notably, the CV risk and its association with kidney function is independent of traditional CV risk factors. Thus, there are kidney-specific mechanisms contributing to the increased CV risk.

Cardiovascular risk factors in CKD

Hypertension is a strong risk factor for the development of CKD. Also, it is a consequence of declining renal function, as it becomes increasingly difficult for the deteriorating kidney to maintain AP within normal limits. Approximately 80 % of patients with CRF are hypertensive,[34] and there is an evident increase in CV risk in hypertensive patients with CKD, compared to normotensives with CKD.[35] Possible mechanisms causing elevated AP in these patients are increased activity of the sympathetic nervous system, increased RAS activity, and endothelial dysfunction.[36-38] The latter may involve decreased bioavailability of NO,[38-40] increased levels of EDCFs, such as endothelin,[41] and increased levels of oxidative stress.[42] In addition, with

declining GFR it becomes increasingly difficult for the kidneys to maintain normal extracellular fluid volume.

Hypertension plays a major role in the induction of left ventricular hypertrophy (LVH) that is usually found already in early stages of CKD.[43-45] The prevalence of LVH is approximately 70 % in patients starting dialysis.[46] Furthermore, it is an independent predictor of survival in ESRD,[47] and associated with an increased risk for sudden cardiac death.[48] Apart from hypertension, renal anemia and increased arterial stiffness also seem to contribute to development of LVH in CKD.[49-53]

Increased aortic stiffness has proven to be a powerful predictor of CV mortality in ESRD, as well as in patients with normal kidney function.[54-55] A consequence of increased aortic stiffness is increased left ventricular afterload, which increases myocardial oxygen consumption, and reduces coronary perfusion, paving the way for myocardial ischaemia.[56]

Previous studies have shown that increased arterial stiffness in CKD patients is correlated to structural remodelling of the vascular wall, e.g., increased intima-media thickness,[57-58] and vascular calcification.[59-60] The kind of calcifications that are usually found in patients with CKD are located in the media of the arterial wall.[61-62] In contrast to atherosclerotic calcifications, also known as plaques, media calcifications do not involve lipid and cholesterol deposits in the intima, but instead consist of VSM calcium deposits, and the production and expression of proteins that are usually involved in the formation of bone.[62]

The initiation process of medial calcification is not well understood, however it is associated with the bone-mineral disorders that develop in CKD.[63-64] A declining kidney function results in decreased production of active vitamin D and reduced elimination of phosphate, which leads to elevated levels of phosphate and parathyroid hormone (PTH) in the blood. In vitro studies on VSMCs show that elevated extracellular calcium and phosphate levels may stimulate phenotypic changes that predispose to calcification.[64-66]

Thus, there are many risk factors that are associated with CV mortality in patients with CKD. However, there is a gap in knowledge regarding the initiating mechanisms for these risk factors. The coexistence of renal dysfunction and traditional CV risk factors in CKD patients makes it difficult

to study kidney-specific effects on the CV system. Animal models, however, allow for investigation of clinical observations within a controlled environment.

2 AIMS

The overall aim of this thesis was to clarify the pathophysiological mechanisms that contribute to increased CV risk in CRF.

The specific aims of the papers included in this thesis were

I. To develop a model of adenine-induced chronic renal failure (A-CRF) in rats and to examine arterial pressure and the effects on mesenteric resistance arteries and the thoracic aorta.

II. To investigate whether the reduced aortic relaxation rate observed in paper I is associated with aortic stiffness in A-CRF rats and to investigate the pathophysiological mechanisms by which hypertension develops in this model.

III. To investigate the presence of reduced relaxation rate in different conduit arteries of A-CRF rats and to elucidate mechanisms responsible for this vascular abnormality through gene expression analyses.

IV. To investigate the effects of a high NaCl intake on arterial functions and aortic relaxation rate in A-CRF rats.

.

3 METHODS

The following is a brief overview of the methods used in this thesis. More detailed descriptions of materials and methods are found in each paper.

3.1 General procedures

All animal procedures were approved by the regional ethics committee in Gothenburg, Sweden.

A total of 419 male Sprague-Dawley rats (Harlan Horst, the Netherlands and Charles River, Germany) weighing ~300 g were included in studies I-IV. Rats were housed in rooms with a controlled temperature of 24-26°C and a 12:12-h dark-light cycle.

3.2 A model of chronic renal failure

The most commonly used experimental models of CRF rely on surgical interventions. Many of them involve nephrectomy, the removal of renal mass, either by excision or infarction. Establishing a model that involves surgical techniques is time consuming, as there are large inter-individual and inter-laboratory variations due to the fact that progression of renal failure is dependent on the amount of tissue removed or infarcted.[67] In addition, there are risks of surgical and anesthetic complications affecting mortality rates. A widely used model of CRF, especially in rats, is 5/6 nephrectomy. It involves removal of an entire kidney, followed by either infarction or surgical removal of approximately 2/3 of the remaining kidney. Because of the ensuing hyperfiltration of the remaining renal mass, it usually takes up to several months for CRF to develop in the 5/6 nephrectomy model.[68]

To circumvent the abovementioned obstacles we employed a model of A-CRF in rats. Adenine is an organic compound that acts as one of the building blocks of DNA, and is an important component of various biomolecules. It is generally metabolized by adenine phosphoribosyltransferase, an enzyme widely expressed is mammalian cells. However, an excess of adenine will lead to degradation via xanthine oxidase resulting in 2,8-dihydroxyadenine (DHA),[69] a metabolite that is freely filtered in the glomeruli. Due to the low

solubility of DHA it precipitates once it reaches the renal tubules, at the psyiological pH of urine,[70] thereby causing tubular obstruction which then leads to renal failure.

The renal failure in this model, compared to the 5/6 nephrectomy model, is more severe,[71] and produces disordered mineral metabolism and secondary hyperparathyroidism. A-CRF also produces a uniformly distributed tissue damage of the kidneys, which resembles the clinical phenotype of patients with CKD. One of the drawbacks with this model is that renal failure is caused by an exogenous substance, a scenario that does not usually occur amongst patients. Another drawback is that rats find adenine-containing chow rather unpalatable and, as a consequence, tend to lose a significant amount of weight at the conventionally used adenine concentration of 0.75% in the diet.[72-73] However, this can be avoided by lowering the concentration of adenine over time, or maintaining a low concentration throughout the study.[74-75]

3.2.1 Feeding protocols

CRF was induced by feeding a standard pelleted chow containing adenine. To avoid major weight loss of animals the diet provided consisted of 0.5% adenine the first 3 weeks, 0.3% the following 2 weeks and 0.15% thereafter. Control rats were fed an identical chow without adenine through pair-feeding, a method used to match food intake and body weights (BW) between different groups. Figure 2 shows the effects of reducing adenine concentrations and pair-feeding on BW and water intake.

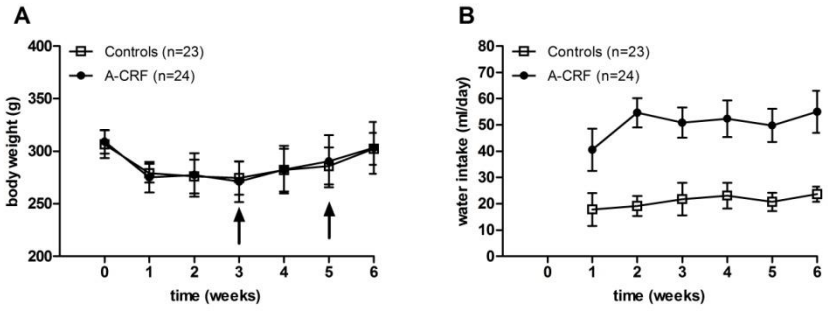

Figure 2. Weekly monitoring of body weights (A) and water intake (B) in rats with adenine-induced chronic renal failure (A-CRF) and controls. No significant differences in body weights were found between groups, a result from pair-feeding control rats. Arrows indicate time points when concentrations of adenine in the chow were reduced in A-CRF group. Rats started gaining weight after the first reduction of adenine concentration. Water intake in A-CRF rats elevated two-fold after the first week of adenine intake, compared to controls, which was also accompanied by an increased urine output, indicative of tubular damage. Figure from paper I.

In papers III and IV rats were randomized into 4 groups 2 weeks before sacrifice. Rats either remained on the same diet with normal NaCl content (0.6%) or were switched to an identical diet with high NaCl content (4%). A schematic illustration of the feeding protocol and time of experimental procedures is shown in Figure 3.

Figure 3. Schematic illustration of study protocol.

3.3 Kidney function and fluid-handling

Creatinine clearance (C_{Cr}) is a widely used clinical method for measuring GFR.[76] Skeletal muscle creatine is metabolized into creatinine,[77] a waste product that is rapidly eliminated by the kidneys. Thus, high serum creatinine levels indicate loss of renal function. For estimation of C_{Cr}, determination of creatinine levels in both serum and timed urine collections are needed.

Rats were placed individually in metabolic cages (papers II and III) for 3 consecutive days. On the third day, BW, water intake and 24-hour urine collections were obtained, and blood was sampled from the tail vein.

3.4 Blood pressure measurements

3.4.1 Tail cuff plethysmography

Tail cuff plethysmography is a non-invasive method for measuring AP. For study IV a light-based plethysmographic method, in which a light source illuminates a small spot on the tail in attempt to record pulse during deflation of an occlusion cuff on the tail, was used. The method requires no surgical intervention, however it requires training of animals if measurements are to be made while they are awake as they need to be placed in a constrainer, which is rather stressful and causes increased blood pressure. Any movement of the animal will create artifacts on the recordings, thereby making it difficult to obtain proper measurements. This method can also be performed on anesthetized animals, making it easier to perform measurements, however it is important to consider that anesthesia might reduce AP.

Systolic blood pressure (SBP) was measured under light isoflurane anesthesia at weeks 1, 3, 5, 6, and 7 after study start, using tail cuff plethysmography (paper IV).

3.4.2 Radiotelemetry

AP measurements were performed using radiotelemetry, which is the gold standard of measuring AP and HR, as it allows for measurements in freely moving animals. The principle is that a surgically implanted radiotelemetry transmitter monitors AP and HR within the abdominal aorta, through a

catheter, in freely moving animals. The signals are then transmitted to an externally located receiver, transferring these further to a data acquisition system. Compared to the tail-cuff method, radiotelemetry provides much more reliable values and also the possibility to study pressure and HR fluctuations over time. However, this is an expensive method and requires surgical expertise. Surgery is not always successful, and even if it is, it is not always certain that the transmitter will work once it has been placed inside the animal. Also, animals need to be kept individually to reduce risk of transmitters being damaged, thus managing big or many study groups can be difficult and time consuming.

Figure 4 schematically illustrates the radiotelemetry study protocol used for paper I and II.

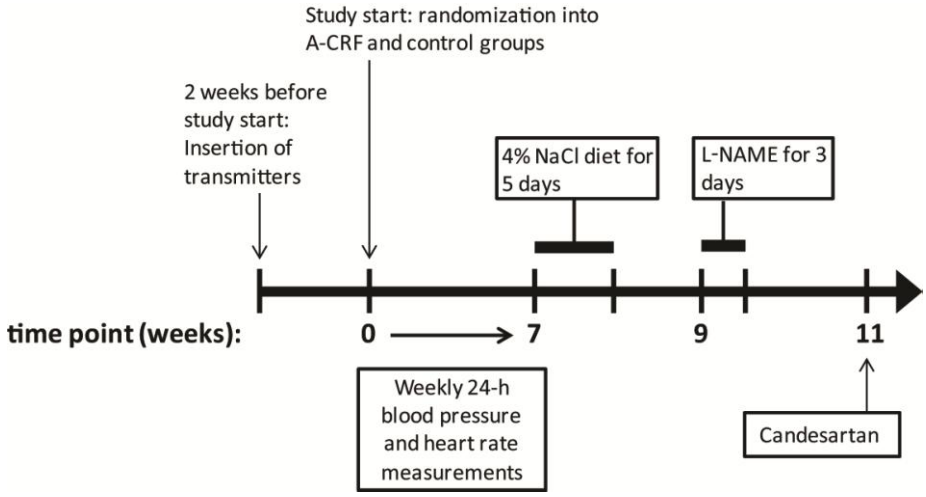

Figure 4. Schematic illustration of experimental setup of radiotelemetry study. Each intervention was followed by at least 1 week wash-out period. L-NAME, Nω-nitro-L arginine-methyl ester hydrochloride.

3.5 Assessment of vascular function ex vivo

Using wire myography, compliance, contractility, and structural and excitation-contraction coupling characteristics of isolated vascular vessels can be studied in a controlled environment.[9] These properties are difficult to study in vivo, because of the many factors that can influence the vascular responses. In this method, a vascular ring segment is mounted onto two steel wires in a myograph chamber filled with physiological salt solution (PSS). The segment length is measured and the chamber heated to 37 °C. The length-tension relation of the vascular segment is determined by a series of step-wise stretching when fully relaxed, and d_{100}, which is the estimated diameter the vessel would have at a transmural pressure of 100 mmHg, is calculated using the Laplace law (Figure 5). For experimental procedures, the diameter was set to 0.9 d_{100}, the diameter at which arterial resistance vessels produce a maximum isometric response.[78] All vessels used were normalized with this setting.

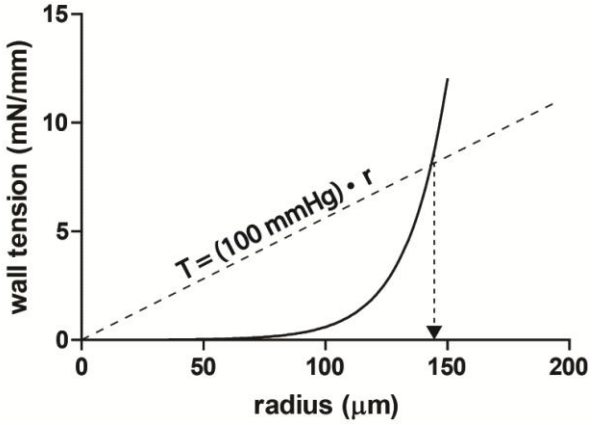

Figure 5. Determining vessel diameter at a given pressure using the law of Laplace. Step-wise stretching of a fully relaxed vessel segment in the myograph is performed for determining the length-tension relation (solid line). The length is presented as the radius (r) of the vessel. The Laplace law states that wall tension (T) of a vessel at a given transmural pressure (P) is $T = P \cdot r$. The length-tension relation of the vessel at a pressure of 100 mmHg is presented by the dashed line. The arrow shows the radius of the vessel when the pressure is 100 mmHg, which is underneath the intersection of the solid and dashed lines.

Normalization is important for a clearly defined condition that facilitates comparison of differently sized vessels, and it is also important due to the fact that the degree of stretch determines the response of the vessel, and thereby the sensitivity to pharmacological agents also.[79]

The vessels used for myography (papers I, III, and IV) were mesenteric arteries, thoracic aorta, abdominal aorta, left common carotid artery and left common femoral artery.

3.6 Assessment of aortic stiffness

Aortic stiffness was assessed by measuring pulse-wave velocity (PWV), which is considered to be an independent and powerful predictor of CV death,[55] not only in patients with renal insufficiency, but also in patients with normal renal function.[80] During the systolic phase the left ventricle ejects blood and each ejection generates a pressure wave, a pulse, that is propagated along the vasculature for delivery of oxygen and nutrients to different tissues. The rate at which pressure waves move away from the heart down a vessel is the PWV (Figure 6).

Decreased aortic compliance results in increased PWV as the aorta distends less in response to the pressure wave, thereby causing it to travel much faster through the vessel. In addition, reflected waves, generated at arterial branching points, will also be propagated at an increased velocity. An early return of reflected waves augments the systolic part of the forward pressure wave, thus elevating SBP further.[81] The augmented systolic part of a pressure wave is known as augmentation index (AI).

Isoflurane-anesthetized rats were used for PWV measurements. Apart from measuring aortic AP the pressure sensors were also used for measuring left ventricular end-diastolic pressure (LVEDP) by advancing the catheter further.

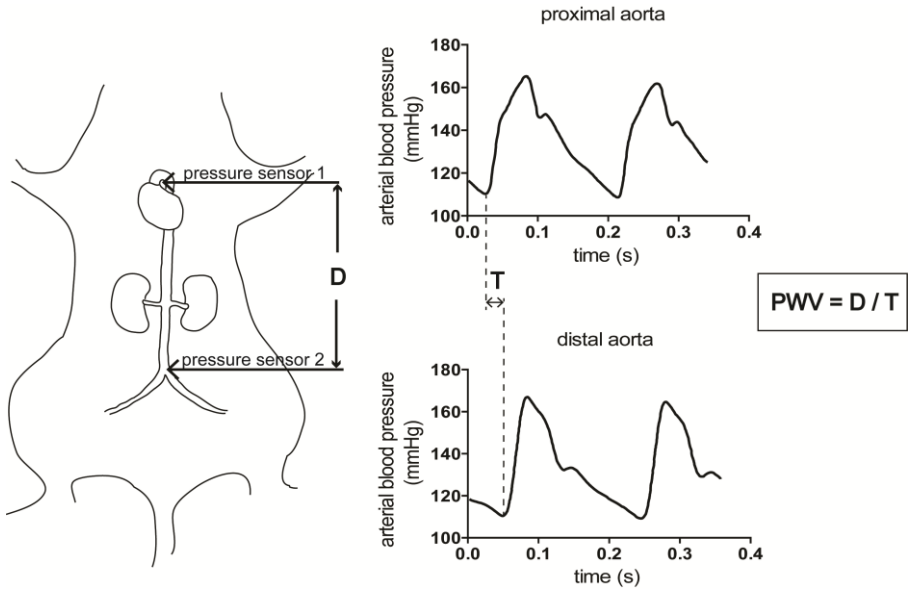

Figure 6. Assessment of aortic stiffness by measuring aortic pulse-wave velocity (PWV) in rats. Pressure sensor 1 is placed immediately above the aortic valve through the left carotid artery and pressure sensor 2 is placed at the level of the aortic bifurcation through the right femoral artery. PWV is equal to the time (T) it takes for one pressure wave to travel from the first to the second pressure sensor divided by the distance (D) between the two transducers. Arterial pressure is also measured at the two sites for estimating augmentation index (AI), a measure of pressure wave reflection. Modified figure from Cosson et al.[82]

3.7 Histological analyses

Sections of mesenteric arteries and aortic rings used in myograph studies were prepared and stained with either hematoxylin and eosin, or von Kossa staining (I) for visualization of tissue calcifications. Hematoxylin and eosin-stained sections were used for quantification of the cross-sectional area and thickness of the intima-media, and vessel lumen radius.

3.8 Gene expression analyses

3.8.1 Microarray

Microarray technology is used for mapping gene expressions of tissues. RNA from a tissue sample is copied and labelled with biotin. Short, single-stranded DNA molecules, also known as oligonucleotides, attached to a microchip, are hybridized with the biotinylated complementary RNA. The biotin binds streptavidin, a marker that fluoresces under laser light when successful base pairings are made. The fluorescent signals are quantified and gene expression levels are thereby obtained (Affymetrix).

Thoracic aortas were used for microarray analysis (III). From the microarrays, 117 genes were preselected to be included in the study. These genes were selected based on the known importance of their gene products in regulating excitation-contraction coupling in VSMCs of large arteries.

3.8.2 Quantitative real-time polymerase chain reaction

Microarray data was verified using quantitative real-time polymerase chain reaction (qRT-PCR), in which the synthesis and real-time detection and quantification of specific DNA fragments are made from RNA samples. Through a series of repetitive cycles of denaturation, hybridization, and polymerase extension, DNA fragments are doubled during each cycle and thereby exponentially increased.

3.9 Plasma measurements

Plasma and urine creatinine levels were measured using a photoenzymatic assay and calcium and phosphate were photometrically quantified. Plasma and urine concentrations of potassium and sodium were measured using an ion selective electrode. Intact PTH was analyzed by an enzyme-linked immunosorbent assay (ELISA), and plasma renin activity (PRA) and aldosterone analyses were performed using radioimmunoassay kits. L-arginine (L-arg), and asymmetric (ADMA) and symmetric (SDMA) dimethylarginine in plasma were measured with high-performance liquid

chromatography (HPLC). Total plasma malondialdehyde (MDA) was measured using HPLC and fluorescence detection. Mass spectrometry was used for quantifying 8-hydroxy-2-deoxyguanosine (8-OHdG). Plasma nitrite concentrations were quantified by chemiluminescence.

4 REVIEW OF RESULTS

The following is a brief overview of the main results found in each paper.

Renal function, fluid-handling and metabolic disorders in A-CRF

We found, in paper I, that rats with A-CRF develop marked elevations in plasma creatinine levels already at two weeks after study start, compared to controls (Figure 7).

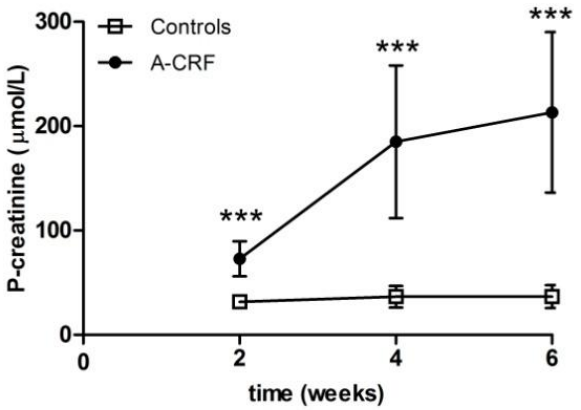

*Figure 7. Creatinine levels of plasma sampled from the tail vein at 2, 4 and 6 weeks after study start. n = 7 per group. Data presented as means ± SD. ***P<0.001. Figure from paper I.*

At time of sacrifice the creatinine levels had increased to ~8-fold of control values (Table 1). C_{Cr} measurements, performed at both 9 and 12 weeks after study start (papers III and II, respectively), were in A-CRF rats approximately 10-12 % of control values. A marked increase in urine output (3- to 4-fold compared to controls) and a corresponding elevation in water intake (P<0.001) were found also.

Rats with A-CRF had increases in left ventricular mass and increased plasma levels of calcium, phosphate, potassium, aldosterone and PTH (Table 1). Levels of hemoglobin and 1,25-dihydroxyvitamin D_3 were significantly

reduced. A-CRF rats also had marked reductions in levels of PRA. No significant differences were found in plasma sodium levels between groups.

Table 1. *Left ventricular weight and blood analyses at time of sacrifice*

	Controls	A-CRF
LVW/tibia length (g/mm)	17.5 ± 1.4	20.9 ± 2.3***
Hb (g/l)	162 ± 5	118 ± 14***
P-creatinine (µmol/L)	28 ± 3	234 ± 83***
P-calcium (mmol/L)	2.6 ± 0.1	2.8 ± 0.2**
P-phosphate (mmol/L)	2.2 ± 0.2	2.8 ± 0.4***
P-potassium (mmol/L)	6.1 ± 0.7	7.2 ± 0.7***
P-sodium (mmol/L)	142 ± 1	141 ± 2
P-aldosterone (pmol/L)	601 ± 410	1610 ± 689**
P-PTH (pg/mL)	120 ± 56	783 ± 418***
PRA (µg/L/h)	6.5 ± 2.6	0.7 ± 0.5***
P-1,25-dihydroxyvitamin D_3 (pg/mL)	76 ± 23	29 ± 10***

Animals were sacrificed at 6-12 weeks after study start. For PRA, PTH, 1,25-dihydroxyvitamin D3 and aldosterone n = 6-11 per group, otherwise *n* = 15-24 per group. Hb, hemoglobin; LVW, left ventricular weight; P, plasma; PRA, plasma renin activity; PTH, parathyroid hormone. Values are means ± SD. **P < 0.01,***P < 0.001. Data from paper I.

When fed a high NaCl diet for two weeks (paper IV), rats with A-CRF had significantly increased BW, right ventricular mass, and augmented LVH. Lung water content was significantly increased as an effect of adenine in this study. Plasma sodium levels were significantly increased by high NaCl intake in A-CRF rats, with an approximate 1 mM increase. In addition, plasma creatinine levels of these rats were significantly lower compared to those receiving adenine diet with normal NaCl intake.

Hypertension in A-CRF

In paper I, moderate hypertension was found in rats with A-CRF (Figure 8). In addition, A-CRF rats had significantly decreased HR. The onset of hypertension occurred after 2 weeks of adenine diet.

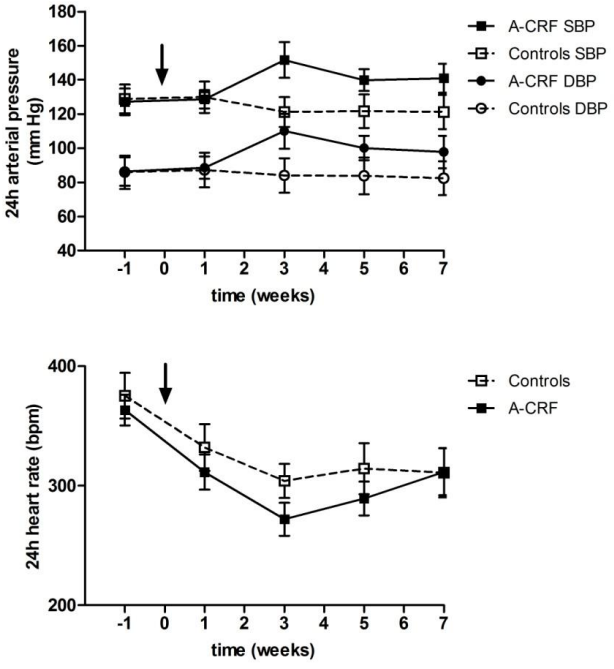

Figure 8. Measurements of arterial pressure and heart rate in conscious rats using radiotelemetry. Arrows indicate the time-point of randomization of rats to either adenine-containing chow or normal control diet. DBP, diastolic blood pressure; SBP, systolic blood pressure. Values are means ± SD. Figure from paper I.

The underlying mechanisms causing the hypertension in A-CRF were investigated in paper II, by measuring the effects of a high NaCl intake, NOS inhibitor Nω-nitro-L arginine-methyl ester hydrochloride (L-NAME), and Ang II receptor antagonist candesartan on AP and HR (Figure 9).

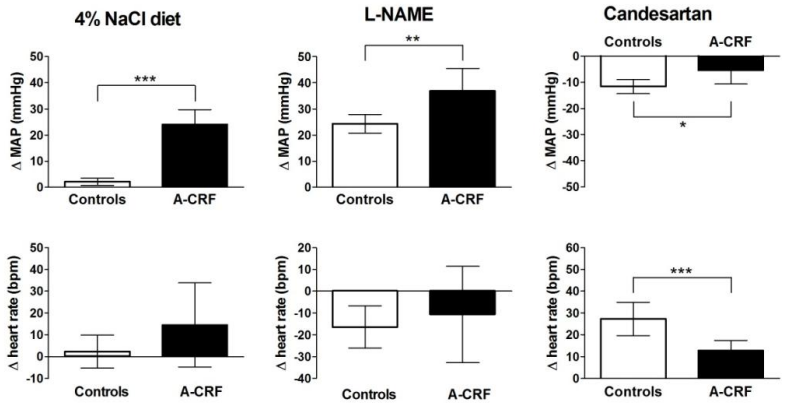

*Figure 9. Changes in mean arterial pressure (MAP) in response to 4% NaCl diet, L-NAME and candesartan. Baseline values were compared with day 5 of 4% NaCl diet, day 3 of L-NAME treatment and day 1 following a single dose of candesartan. Data are expressed as means ± SD. *P<0.01, **P<0.01, ***P<0.001. Figure from paper II.*

MAP was significantly increased in rats with A-CRF compared to controls during a 5-day intake of a high NaCl diet, whereas HR did not differ between groups. During this period, significant increases in BW were observed in A-CRF rats. Inhibition of L-NAME produced increases in MAP in both groups, however the increase was significantly more pronounced in A-CRF rats. Additionally, HR levels were reduced in a similar manner in both rats with A-CRF and controls, with no significant differences between the two. MAP was significantly reduced in response to candesartan in both groups, with a reduction that was significantly more pronounced in control rats than in rats with A-CRF. The concomitant increase in HR was significantly more prominent in controls vs. A-CRF group.

Endogenous NOS inhibitors ADMA and SDMA were significantly increased in plasma of A-CRF rats compared to controls, however, concentrations of NO precursor L-Arg and NO marker plasma nitrite (P-nitrite) were not significantly different between groups (paper I). Plasma levels of oxidative stress markers MDA and 8-OHdG were significantly elevated in A-CRF group vs. controls.

Aortic stiffness and diastolic dysfunction

In paper II, assessment of aortic PWV revealed a significant increase in rats with A-CRF compared to controls at baseline, and during infusion of SNP, but not during phenylephrine (PE) administration (Figure 10). Measurements of AP revealed significantly increased AIs in A-CRF group, both in the ascending aorta ($P<0.05$) and at the level of the aortic bifurcation ($P<0.05$).

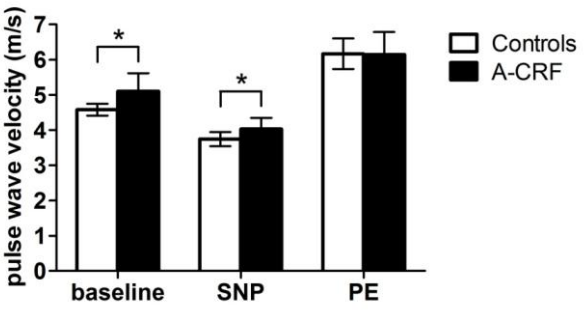

*Figure 10. Aortic pulse wave velocity measured in isoflurane-anesthetized rats at baseline and during infusion of sodium nitroprusside (SNP) and phenylephrine (PE). Mean arterial pressure was significantly increased in A-CRF group at baseline (P<0.05), but not during infusion of SNP and PE. n = 10 per group. Data are expressed as means ± SD. *P<0.05. Figure from paper II.*

LVEDP measured at baseline conditions was almost doubled in rats with A-CRF in comparison to controls.

Vascular dysfunction in A-CRF

In paper I, we found that thoracic aortas from A-CRF rats with normal NaCl intake exhibited a reduced rate of relaxation, mainly in response to wash-out of KCl (Figure 11), but also in response to vasodilators acetylcholine (ACh) and sodium nitroprusside (SNP). No significant alterations in response to concentration-response relations of α-adrenergic agonists or ACh and SNP were found in either mesenteric arteries or the aorta. Reduced relaxation rates were also found in the common carotid artery and the abdominal aorta of rats with A-CRF (paper III).

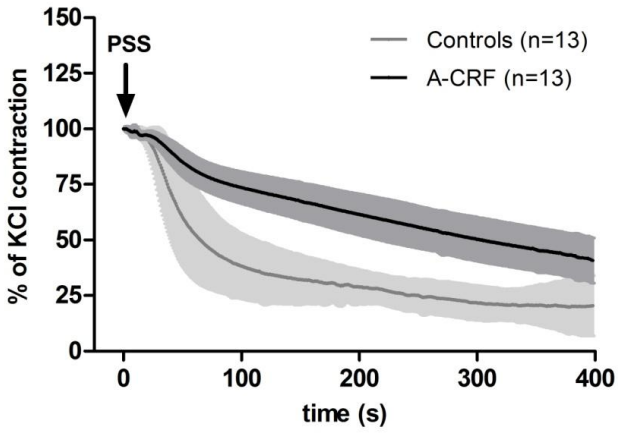

Figure 11. Time course of aortic relaxation after wash-out of 125 mM KCl with physiological salt solution (PSS). Full lines represent means and shaded areas represent SD. Figure from paper I.

In paper IV, a decreased sensitivity in response to NE was found in mesenteric arteries of A-CRF rats that had been on a high NaCl diet for 2 weeks. The neuronal reuptake inhibitor, cocaine, produced similar shifts in the concentration-response relations for NE in all groups. In the thoracic aorta of A-CRF rats high NaCl intake aggravated the decrease in relaxation rate further and significantly decreased the sensitivity to both ACh and SNP. In addition, basal vascular tone was elevated in the presence of calcium.

Investigating mechanisms causing reduced rate of aortic relaxation

Functional analyses

The reduced relaxation rate in A-CRF thoracic aortas still remained after removal of endothelium (paper I and III) and extracellular calcium (paper III). This ruled out endothelial dysfunction and leakage of extracellular calcium into the cytosol as possible causes of the impairment in vasorelaxation. Indirect quantification of calcium levels in intracellular stores was made by quantifying contractile response of aortic rings to PE in a calcium-free environment until vessels no longer responded. Aortas from A-CRF rats responded significantly less compared to controls, indicating that calcium levels in the SR may be reduced. Concentration-response relations to

both calcium and KCl were performed, showing no differences in sensitivity between rats with A-CRF and controls.

Gene expression analyses

Gene expression analyses of thoracic aortas were performed to gain better insight of the molecular changes that occur in the aorta of A-CRF rats. From our microarray analysis in paper III, the expression of 15 genes were further verified using qRT-PCR. The genes that will be discussed are listed in Table 2.

Table 2. *Aortic gene expression by qRT-PCR*

Gene	Description	Expression (A-CRF vs. controls)
Atp1α2	α_2-subunit of NKA	↓
Atp2α2	SERCA2	↓
Casq1	calsequestrin 1	↑
Casq2	calsequestrin 2	↑
Pln	phospholamban	↑
Ppp1r14a	CPI-17	↑
Stim1	stromal interaction molecule 1	↓
Trpc4	transient receptor potential cation 4	↑

Significantly upregulated (↑) and downregulated (↓) genes in A-CRF thoracic aortas. CPI-17, C-kinase potentiated protein phosphatase-1 inhibitor 17 kDa; NKA, Na,K-ATPase; SERCA, sarcoendoplasmic reticulum calcium ATPase.

Vascular compliance and morphology

No differences were found in vascular compliance between groups when assessed ex vivo, even though morphological analysis revealed that rats with A-CRF had a significantly increased media thickness (Figure 12) and media-to-lumen ratio in thoracic aortas. Decreases in aortic wall tension and wall

stress were found also. Media thickness in aortas was further increased in response to a high NaCl intake in paper IV. Aortic media calcifications were detected only in 1 animal used for PWV analysis in paper II. No vascular calcifications were detected in any of the other vessels included in the papers of this thesis.

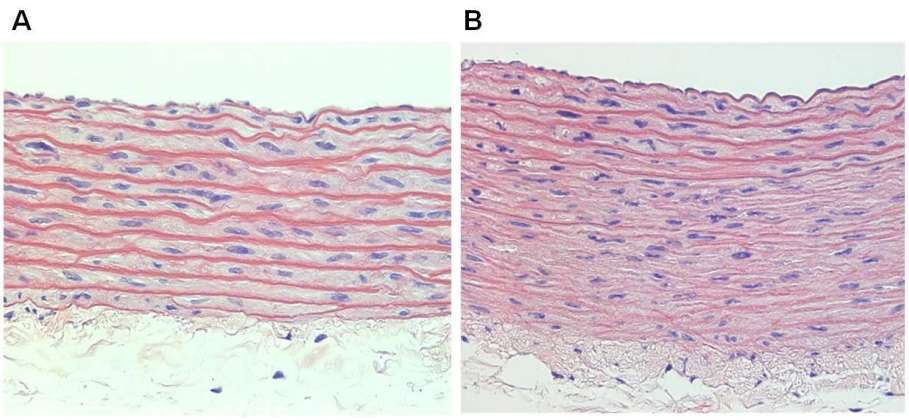

Figure 12. Morphology of thoracic aortas from control (A) and A-CRF group (B) at 40x magnification. The medial layer of aortas from A-CRF rats displayed fragmentation of elastic lamellae and disorganization of vascular smooth muscle cells. This was found in 7 out of 13 animals. Sections were stained with hematoxylin and eosin. Figure from paper I.

5 DISCUSSION

The kidney-specific effects of dietary adenine in rats were first described in the literature in 1986,[83] and adenine has frequently been used to study the effects of renal failure on bone-mineral metabolism and mechanisms of vascular calcification.[72, 84-88] In this thesis, we used this model for investigating the effects of renal insufficiency on the cardiovascular system, in an attempt to elucidate mechanisms that contribute to the increase in CV risk in patients with CRF.

Kidney function in A-CRF

Rats with A-CRF developed pronounced reductions in GFR already at 2 weeks after study start. C_{Cr} measurements indicated that GFR was reduced to approximately 10 % of control values. Thus, at the time of ex vivo studies of vascular function, A-CRF rats had already been exposed to at least 4 weeks of severe renal failure. Furthermore, rats with A-CRF also developed metabolic abnormalities characteristic of patients with CRF, such as hyperphosphatemia, secondary hyperparathyroidism, hyperkalemia and renal anemia. Thus, A-CRF in rats closely resembles the clinical syndrome of uremia in patients.

A-CRF induces hypertension

Rats with A-CRF developed moderate elevations in AP that was accompanied by a significant baroreceptor-mediated decrease in HR. However, at week 7 after study start, the difference in HR between groups was eliminated, despite sustained AP elevation in A-CRF rats. This suggests that rats with A-CRF develop impaired baroreceptor function, which further stresses the clinical relevance of the A-CRF model, as studies have shown that baroreceptor dysfunction is present in patients with CRF.[89-90] In a previous study of ours,[91] we found that rats with A-CRF had a markedly reduced baroreceptor sensitivity after 10-12 weeks of renal insufficiency. The link between hypertension and the development of baroreceptor dysfunction is well-described in the literature,[92] and decreased baroreceptor sensitivity has been found to be an independent predictor of sudden cardiac death in patients with CRF.[93]

AP levels were further increased when A-CRF rats were exposed to a high NaCl intake for 5 days, and this was associated with more pronounced increases in BW compared to controls. These results suggest that the AP elevation in response to high NaCl diet in A-CRF is likely to be caused by sodium retention and extracellular fluid volume expansion. In addition, the high NaCl-induced increase in AP was accompanied by an increase in HR whereas L-NAME-induced hypertension resulted in decreased HR, again indicating an impaired baroreflex, especially during high NaCl intake in A-CRF rats. Also, the elevated AP in A-CRF rats did not appear to be caused by the RAS, as the Ang II receptor antagonist candesartan only produced minor reductions in MAP, compared to control rats. This was supported by measurement of PRA, which was significantly suppressed in A-CRF rats.

We speculated that the elevated AP may have been a consequence of NO deficiency in rats with A-CRF. In 1992, Vallance et al[94] reported that patients with ESRD have increased levels of the endogenous NOS inhibitor ADMA, leading to inhibition of NO synthesis. SDMA, another dimylethylarginine, interferes with NO synthesis by competing with the NO precursor L-arg for transmembrane transport.[95] Both of these are eliminated through renal excretion,[96] explaining the elevated plasma levels of ADMA and SDMA in patients with CRF.[94, 97] We found that plasma levels of ADMA and SDMA in rats with A-CRF were significantly elevated compared to controls. NO availability was estimated by measuring the concentrations of P-nitrite and L-arg. Results showed that these markers did not differ between groups, although P-nitrite levels tended to be reduced in A-CRF rats. In addition, oxidative stress markers MDA and 8-OHdG were significantly increased in this group. Increased levels of oxidative stress markers in patients with CRF have been correlated to an impaired endothelial-dependent vasodilation,[98] most likely through the inactivation of NO.[99] Several investigators have demonstrated that both acute and chronic inhibition of NOS induces arterial hypertension in animal models.[100-103] Somewhat surprisingly, inhibition of NOS by L-NAME produced a more pronounced AP increase in A-CRF rats compared to controls. This finding suggests that NO production may be compensatory upregulated in A-CRF rats to attenuate hypertension.

Effects of a high NaCl intake

A two-week period of high NaCl intake caused significant increases in BW of A-CRF rats, and we also observed fluid accumulation in the chest and abdominal cavities. These results indicate that high NaCl intake in A-CRF increases total body sodium and cause extracellular fluid volume expansion. Additionally, plasma sodium levels were significantly increased in rats with A-CRF, by a slight 1 mM. Studies have demonstrated that increased plasma sodium concentrations are associated with increased levels of endogenous ouabain (EO),[104-106] a substance that is believed to promote natriuresis by inhibiting tubular sodium reabsorption.[107-110] In addition, EO can cause vasoconstriction and hypertension. The details of this mechanism will be discussed further ahead in this discussion. There is a possibility that increased AP in response to high NaCl intake may have been partially mediated by EO.

LVH was augmented by high NaCl intake in A-CRF rats, which is in agreement with our AP findings. Increases in RV mass were also observed, suggesting pulmonary hypertension, most likely caused by the augmented LVH and left ventricular diastolic dysfunction. Taken together, these findings clearly demonstrate that high NaCl augments CV risk factors in A-CRF.

Increased aortic stiffness is not caused by vascular calcification

We found that rats with A-CRF had an increased aortic stiffness compared to control animals, which was not caused by vascular calcifications. Pulse wave analysis also revealed that reflected pulse waves in A-CRF rats contributed more to aortic pulse pressure and SBP, than in controls. Thus, elevated aortic SBP caused by increased aortic stiffness may likely have contributed to LVH in A-CRF, as aortic stiffness leads to increased left ventricular afterload. In support of this, an increased LVEDP was found in A-CRF, a consequence of either decreased compliance of the left ventricle or impaired relaxation. Important to consider is that the degree of arterial stiffness varies with MAP, e.g., an increased MAP correlates with increased arterial stiffness.[111] Because of this, differences in MAP between groups were eliminated by the infusion of SNP and PE. During infusion of SNP aortic stiffness was still increased in A-CRF rats, despite similar MAP as controls. These findings suggest that increased arterial stiffness in A-CRF develops independently of vascular calcification and increased MAP. We can, however, not rule out the

possibility that hypertension may contribute to the development of increased arterial stiffness in CRF.

Vascular structure and function A-CRF

Despite severe renal failure, mesenteric resistance arteries from rats with A-CRF did not show any structural or functional differences compared to controls. When fed a high NaCl diet for 2 weeks, a decreased NE sensitivity was found in the A-CRF group, but this was the only abnormality observed.

In a study performed by Mulvany et al.,[112] the degree of sympathetic nerve activity in spontaneously hypertensive rats (SHR), compared to control Wistar Kyoto rats (WKY), were investigated by comparing differences in sensitivity to NE before, and during, inhibition of neuronal reuptake of NE, using neuronal reuptake inhibitor cocaine. They found that mesenteric arteries of SHR compared to WKY had more pronounced increase in sensitivity to NE in the presence of cocaine, indicating an increased sympathetic innervation on these vessels. We performed a similar experiment in mesenteric arteries, and found that the responses were similar between groups, suggesting that neither renal failure, nor 2 weeks of elevated NaCl intake, affected sympathetic innervation of mesenteric resistance arteries.

Other investigators have previously been able to demonstrate the presence of endothelial dysfunction,[113-114] and structural remodelling characterized by increased intima-media thickness and decreased vessel lumen of resistance arteries in experimental CRF.[113, 115] We cannot determine the reason for this discrepancy. However, a possible explanation could be that hypertension often has been more severe in other experimental CRF models.[114-115]

Thoracic aortas from rats with A-CRF had a markedly reduced relaxation rate, a finding that is likely linked to increased aortic stiffness. This vascular abnormality was restricted to the major conduit arteries proximal to the common femoral artery, suggesting that the uremic milieu *per se*, was not responsible for the relaxation defect. Still, one might speculate that hypertension was a major cause of the decrease in relaxation rate of large arteries observed in A-CRF rats. We addressed this issue in a pilot study in which A-CRF rats were either treated with antihypertensive drugs or untreated. Interestingly, antihypertensive therapy had no significant effects on aortic relaxation rate although AP was successfully treated to almost

control levels. Thus, hypertension in itself does not seem to cause reduced relaxation rate in large conductance arteries of rats with A-CRF.

In contrast to previous studies in experimental CRF models, we did not find any endothelial dysfunction in A-CRF aortas. This might have to do with the fact that some of the previous studies of experimental CRF used the 5/6 nephrectomy model by renal infarction,[116-117] which is characterized by an active RAS during the early phases of hypertension development.[118-119] Ang II has been shown to impair endothelial function in several studies,[120] and Ang II receptor blockers have demonstrated improvement of endothelial function in patients.[121-123] Another possible explanation could be that we did not find any calcifications in our model. Some of the previous experimental studies that were able to demonstrate endothelial dysfunction used higher concentrations of phosphate and calcium in the diet to induce calcifications.[117, 124] In a study by Diwan et al.,[125] endothelial dysfunction was present in aortas from rats with A-CRF. The duration of renal insufficiency was 16 weeks in that study, however, the authors did not investigate for calcifications. Notably, 2 weeks high NaCl intake further slowed the reduced aortic relaxation rate and induced decreased sensitivity to both ACh and SNP in aortas of A-CRF rats, indicating that VSMCs had a an impaired ability to relax. This does not rule out the possibility that a high NaCl intake in A-CRF rats might also have caused endothelial dysfunction.

Arteries that exhibited a reduced rate of relaxation also had increased media thickness-to-lumen radius ratios. The media thickness-to-lumen radius ratio was further enhanced by a high NaCl intake in A-CRF thoracic aortas. ESRD patients with chronic hypervolemia are subjected to arterial remodelling, especially of the major conduit arteries.[57] In addition, studies on experimental CRF demonstrate that increased wall thickness of aortas is a result of an increased number of VSMCs and increased extracellular matrix that is characterized by an increased collagen content, leading to decreased vascular compliance.[126] The nature of the underlying stimulus for an increased production of extracellular matrix is not clear, although Ang II seems to be involved in the activation of the collagen type 1 gene in aorta,[127] implying that the RAS may be responsible in the initiation process of decreased vascular compliance. We did not find decreased vascular compliance in any of the examined vessels, possibly because of reduced RAS activity in rats with A-CRF, thereby ruling out the possibility that extracellular matrix changes are responsible for the reduced rate of relaxation in A-CRF.

Differentially expressed genes in the thoracic aorta

Thoracic aortas from rats with A-CRF had decreased contractility, which was indicated by decreased wall tension and wall stress. A possible explanation for this could be that expression of CPI-17 (Ppp1r14a) was downregulated in A-CRF thoracic aortas. Previous studies have demonstrated that downregulation of this MLCP inhibitor results in decreased VSM contractility,[128] whereas upregulation enhances contractility.[129]

Functional studies revealed that VSMCs of thoracic aortas from A-CRF rats may have reduced levels of intracellular calcium in the SR, as we observed a greater contractile response in control aortas when eliciting store-induced contractions in a calcium-free environment. In support of this, gene expression analysis demonstrated downregulation of SERCA2 (Atp2α2) and upregulation of its inhibitor phospholamban (Pln). This implies that during the aortic relaxation process calcium levels may not be fully restored in the SR and the levels of cytosolic calcium remain elevated, which could explain the reduced aortic relaxation rate. Inhibition of SERCA using cyclopiazonic acid has been shown to produce a reduced rate of relaxation following washout of KCl in rat aorta.[130] In conjunction with these findings, expressions of calsequestrin-1 (Casq1) and -2 (Casq2) were upregulated in aortas from rats with A-CRF. These are the major calcium-binding proteins in the SR. We hypothesize that the increased expression of these proteins may serve the purpose of preventing leakage of calcium into the cytosol by keeping free calcium levels in the SR relatively low, thus favouring calcium uptake into the SR. In addition, A-CRF induced downregulation of stromal interaction molecule 1 (Stim1), a calcium store sensor that translocates into defined junctional SR located close to the plasma membrane, and causes extracellular calcium entry through the calcium release-activated channel (CRAC) by interacting with Orai1, an important component of CRAC.[131] These events then lead to restoration of calcium stores. In a previous study,[132] Stim1-knockout mice demonstrated a decreased calcium store-refilling rate of aortic VSMCs together with reduced responses to α_1-adrenergic stimulation. The results of that study support our hypothesis on reduced levels of calcium in the SR of aortas from rats with A-CRF. Expression of transient receptor potential cation channel 4 (Trpc4) was upregulated, suggesting that extracellular calcium influx may have contributed to the reduced rate of relaxation also. However, TRPC4 channels appear to be more important in

endothelial cell signaling,[133-134] thus their role in this context is somewhat unclear.

Moreover, we found a downregulation of the ouabain-sensitive α_2-subunit (Atp1α2) of NKA in A-CRF thoracic aortas. NKA is coupled with NCX,[135] which strongly suggests that NKA modulates contractility through extrusion of calcium via NCX by lowering intracellular sodium. The overexpression of α_2 in transgenic mice has demonstrated a more rapid aortic relaxation compared to wild type mice.[136] Thus, reduced activity of the α_2 NKA is anticipated to elevate local intracellular sodium, which reduces the activity of NCX and the extrusion of calcium, leading to elevated intracellular calcium levels that contribute to a reduced relaxation rate. It is possible that elevated plasma levels of EO may have caused downregulation of the α_2 NKA in A-CRF rats. A high NaCl intake has been demonstrated to produce increased sodium levels in cerebrospinal fluid (CSF), compared to the levels in plasma, in models of salt-sensitive hypertension.[137-138] Increased CSF sodium levels, in combination with aldosterone, stimulate hypothalamic levels of EO, which causes sympathoexcitatory responses and hypertension.[139-140] Thus, the high aldosterone levels found in A-CRF rats may be contributing to the elevated AP.

6 CONCLUSIONS AND FUTURE PERSPECTIVES

We have found that rats with A-CRF develop severe renal failure accompanied by metabolic disorders that closely resemble the clinical setting of CRF. A-CRF rats develop hypertension that is not renin-dependent and is exaggerated by a high dietary NaCl intake. One of our major findings is that major conduit arteries of rats with A-CRF develop a reduced rate of relaxation independently of vascular calcifications. This vascular abnormality is associated with an increased aortic stiffness. Furthermore, we found that two weeks of high dietary NaCl in A-CRF rats further impairs relaxation of aortic VSMCs and augments CV injury.

The mechanisms behind the reduced rate of arterial relaxation remain to be defined. Our analyses have verified altered expressions of some of the genes that are critically involved in intracellular calcium-handling mechanisms of aortic VSMCs. Quantification of intracellular calcium levels in aortic VSMCs is an important future experiment.

Downregulation of the α_2-subunit of NKA indicates a possible role of EO in our model of CRF. As described earlier, release of EO is stimulated by increased levels of CSF sodium and aldosterone. Possible ways to link high NaCl intake to elevated EO levels would be to relate CSF sodium levels to plasma EO concentrations.

If we find elevated plasma levels of EO in A-CRF rats it would be interesting to examine the effects of inhibition of EO. An approach to achieve this was presented in a study by Huang et al.,[141] in which they found that central infusion of an aldosterone synthase inhibitor prevents increased CSF sodium to activate the release of aldosterone from the hypothalamus, thus reducing sympathetic activity and AP. This method would be useful for determining the EO-mediated contribution of the sympathetic nervous activity in rats with A-CRF.

Further investigations on ways to normalize the reduced rate of relaxation will be performed by the use of pharmacological agents. Studies will also address issues such as whether a low NaCl diet, or low phosphate diet, in A-CRF rats attenuates the vascular defects.

Investigations on the effects of high NaCl intake in A-CRF are ongoing. Microarray analyses of thoracic aortas from controls and A-CRF rats on a high NaCl diet have shown that many of the genes involved in excitation-contraction coupling that were differentially expressed in thoracic aortas of A-CRF rats on normal NaCl intake are even more affected in A-CRF rats on high NaCl intake.

Our findings provide a possible link between CRF and the development of increased aortic stiffness, a powerful risk factor for death in patients with CKD. The increased aortic stiffness is associated with a reduced aortic relaxation rate, a vascular abnormality that is aggravated by high NaCl intake. The exact mechanisms causing the reduced aortic relaxation rate need to be determined in future experiments, although our results indicate a defect in intracellular calcium-handling in VSMCs. A future therapy targeting this functional abnormality would have the potential to attenuate the development of increased aortic stiffness in patients with CKD.

ACKNOWLEDGEMENTS

I would like to extend my sincerest thanks and appreciation to those who, in one way or another, have contributed to this thesis. Some of the people that I want to highlight include:

Associate professor **Gregor Guron**, my main supervisor – you have been a supportive teacher, a steady guide, and provided me with many laughs with your playful sense of humor throughout the years. Thank you for taking me on as a PhD student and for believing in me at times when I doubted myself.

Professor **Holger Nilsson**, my co-supervisor – you have given me so much of your valuable time and advice and shared so many great stories and puns. Thank you for your tremendous commitment and for sharing your profound knowledge in vascular physiology.

All the co-authors – Thank you for great collaborations and all your hard work.

Emman Shubbar – for your incredible efforts in this project and for all your encouragement and fun talks. You entered our lab with perfect timing and I could not have asked for better support and inspiration during my final year.

Elisabeth Grimberg – we never would have managed to perform the pulse wave velocity and pressure measurements without your expertise. Thank you for your help and for your advice and encouragement.

Jaana Lundgren – for all of your help, especially with histology and immunohistochemistry. You are a wonderful colleague to be around and I still cherish our many talks and laughs.

Maria Johansson – for great collaboration on the radiotelemetry study. I would also like to thank you for making me a part of your 'lab family', and for being there for me whenever I needed to talk.

Margareta Jernås – for helping with the microarrays and for all of your helpful advice. It has been a pleasure collaborating with you, and your never-ending enthusiasm always made me smile.

Intawat Nookaew – for your help with the microarray analysis and for fun meetings.

Gerald DiBona – Thank you for your invaluable input on the papers, great encouragement and advice, and for all the great stories.

Mohamed Ibrahim – for your support in technical issues and for helping me scan all those aortas. I would also like to thank you for being my friend and for always taking your time to be there for me.

Christel Jansson – for all your help with practical matters and university administration, and for many fun conversations.

All my colleagues at the Department of Physiology. Special thanks to **Kerstin Ebefors**, **Veronica Golubinskaya**, **Sansan Hua**, **Peidi Liu**, **Peter Micallef**, and **Marcus Ulleryd –** for lots and lots of cake, tea, and laughter; **Olof Arvidsson**, **Matilda Du Rietz**, **Emelie Eliasson**, **Marta Laskowski**, **David Wadsten**, and **Li-Jin Yang –** for making the lab a little crazier and a little more fun during the summers.

People that I have had the privilege to interact with at Wallenberg lab and the Department of Nephrology, especially **Pavlos Kashioulis** and **Aso Saeed**.

My dear friends and fellow PhD students **Sama Sayin**, **Volkan Sayin**, **Linnéa Schmidt** and **Anna Wilhelmson** – for amazing support and encouragement, and for all the fun dinners, movie nights and game nights.

Mom, **dad**, **Teddy**, **Lan**, **Kham**, **Kent**, **Dennis** and **Tim** – thank you for everything that you have done for me and for being there for me.

Filip, the love of my life and my best friend – throughout the years you have always managed to keep me grounded, helped me grow as a person and supported me at all times. Without you by my side none of this would have been possible.

Pebbles – for being my fuzzy little helper.

REFERENCES

1. Wen CP, Cheng TY, Tsai MK, et al. All-cause mortality attributable to chronic kidney disease: a prospective cohort study based on 462 293 adults in Taiwan. *Lancet* 2008; **371**: 2173-2182.

2. Sarnak MJ, Levey AS, Schoolwerth AC, et al. Kidney disease as a risk factor for development of cardiovascular disease: a statement from the American Heart Association Councils on Kidney in Cardiovascular Disease, High Blood Pressure Research, Clinical Cardiology, and Epidemiology and Prevention. *Circulation* 2003; **108**: 2154-2169.

3. Foley RN, Parfrey PS, Sarnak MJ. Clinical epidemiology of cardiovascular disease in chronic renal disease. *Am J Kidney Dis* 1998; **32**: S112-119.

4. Mitsnefes MM. Cardiovascular complications of pediatric chronic kidney disease. *Pediatr Nephrol* 2008; **23**: 27-39.

5. Guyton AC, Hall JE. Textbook of Medical Physiology. 11th ed: Elsevier Saunders; 2006.

6. Bonjour JP, Malvin RL. Stimulation of ADH release by the renin-angiotensin system. *Am J Physiol* 1970; **218**: 1555-1559.

7. DiBona GF. Peripheral and central interactions between the renin-angiotensin system and the renal sympathetic nerves in control of renal function. *Ann N Y Acad Sci* 2001; **940**: 395-406.

8. Price RJ, Skalak TC. Prazosin administration enhances proliferation of arteriolar adventitial fibroblasts. *Microvasc Res* 1998; **55**: 138-145.

9. Mulvany MJ, Aalkjaer C. Structure and function of small arteries. *Physiol Rev* 1990; **70**: 921-961.

10. Folkow B, Neil E. Circulation: Oxford University Press; 1971.

11. Filo RS, Bohr DF, Ruegg JC. Glycerinated Skeletal and Smooth Muscle: Calcium and Magnesium Dependence. *Science* 1965; **147**: 1581-1583.

12. Somlyo AP, Somlyo AV. Signal transduction and regulation in smooth muscle. *Nature* 1994; **372**: 231-236.

13. Sweeney HL, Yang Z, Zhi G, et al. Charge replacement near the phosphorylatable serine of the myosin regulatory light chain mimics aspects of phosphorylation. *Proc Natl Acad Sci U S A* 1994; **91**: 1490-1494.

14. Di Salvo J, Gifford D, Bialojan C, et al. An aortic spontaneously active phosphatase dephosphorylates myosin and inhibits actin-myosin interaction. *Biochem Biophys Res Commun* 1983; **111**: 906-911.

15. Somlyo AV, Somlyo AP. Electromechanical and pharmacomechanical coupling in vascular smooth muscle. *J Pharmacol Exp Ther* 1968; **159**: 129-145.

16. Berridge MJ. Inositol trisphosphate and calcium signalling. *Nature* 1993; **361**: 315-325.

17. Gordienko DV, Bolton TB. Crosstalk between ryanodine receptors and IP(3) receptors as a factor shaping spontaneous Ca(2+)-release events in rabbit portal vein myocytes. *J Physiol* 2002; **542**: 743-762.

18. Eto M, Ohmori T, Suzuki M, et al. A novel protein phosphatase-1 inhibitory protein potentiated by protein kinase C. Isolation from porcine aorta media and characterization. *J Biochem* 1995; **118**: 1104-1107.

19. Koyama M, Ito M, Feng J, et al. Phosphorylation of CPI-17, an inhibitory phosphoprotein of smooth muscle myosin phosphatase, by Rho-kinase. *FEBS Lett* 2000; **475**: 197-200.

20. Cannell MB, Cheng H, Lederer WJ. The control of calcium release in heart muscle. *Science* 1995; **268**: 1045-1049.

21. Somlyo AP, Himpens B. Cell calcium and its regulation in smooth muscle. *FASEB J* 1989; **3**: 2266-2276.

22. Ledoux J, Werner ME, Brayden JE, et al. Calcium-activated potassium channels and the regulation of vascular tone. *Physiology (Bethesda)* 2006; **21**: 69-78.

23. McCarron JG, Walsh JV, Jr., Fay FS. Sodium/calcium exchange regulates cytoplasmic calcium in smooth muscle. *Pflugers Arch* 1994; **426**: 199-205.

24. Furchgott RF, Zawadzki JV. The obligatory role of endothelial cells in the relaxation of arterial smooth muscle by acetylcholine. *Nature* 1980; **288**: 373-376.

25. Davies PF. Flow-mediated endothelial mechanotransduction. *Physiol Rev* 1995; **75**: 519-560.

26. K/DOQI clinical practice guidelines for chronic kidney disease: evaluation, classification, and stratification. *Am J Kidney Dis* 2002; **39**: S1-266.

27. Go AS, Chertow GM, Fan D, et al. Chronic kidney disease and the risks of death, cardiovascular events, and hospitalization. *N Engl J Med* 2004; **351**: 1296-1305.

28. Matsushita K, van der Velde M, Astor BC, et al. Association of estimated glomerular filtration rate and albuminuria with all-cause and cardiovascular mortality in general population cohorts: a collaborative meta-analysis. *Lancet* 2010; **375**: 2073-2081.

29. Kottgen A, Russell SD, Loehr LR, et al. Reduced kidney function as a risk factor for incident heart failure: the atherosclerosis risk in communities (ARIC) study. *J Am Soc Nephrol* 2007; **18**: 1307-1315.

30. Mann JF, Gerstein HC, Pogue J, et al. Renal insufficiency as a predictor of cardiovascular outcomes and the impact of ramipril: the HOPE randomized trial. *Ann Intern Med* 2001; **134**: 629-636.

31. Abramson JL, Jurkovitz CT, Vaccarino V, et al. Chronic kidney disease, anemia, and incident stroke in a middle-aged, community-based population: the ARIC Study. *Kidney Int* 2003; **64**: 610-615.

32. Hemmelgarn BR, Clement F, Manns BJ, et al. Overview of the Alberta Kidney Disease Network. *BMC Nephrol* 2009; **10**: 30.

33. van der Velde M, Matsushita K, Coresh J, et al. Lower estimated glomerular filtration rate and higher albuminuria are associated with all-cause and cardiovascular mortality. A collaborative meta-analysis of high-risk population cohorts. *Kidney Int* 2011; **79**: 1341-1352.

34. Rostand SG, Brunzell JD, Cannon RO, 3rd, et al. Cardiovascular complications in renal failure. *J Am Soc Nephrol* 1991; **2**: 1053-1062.

35. Kokubo Y, Nakamura S, Okamura T, et al. Relationship between blood pressure category and incidence of stroke and myocardial infarction in an urban Japanese population with and without chronic kidney disease: the Suita Study. *Stroke* 2009; **40**: 2674-2679.

36. Hand MF, Haynes WG, Webb DJ. Hemodialysis and L-arginine, but not D-arginine, correct renal failure-associated endothelial dysfunction. *Kidney Int* 1998; **53**: 1068-1077.

37. Kari JA, Donald AE, Vallance DT, et al. Physiology and biochemistry of endothelial function in children with chronic renal failure. *Kidney Int* 1997; **52**: 468-472.

38. Wang D, Iversen J, Wilcox CS, et al. Endothelial dysfunction and reduced nitric oxide in resistance arteries in autosomal-dominant polycystic kidney disease. *Kidney Int* 2003; **64**: 1381-1388.

39. Zoccali C, Bode-Boger S, Mallamaci F, et al. Plasma concentration of asymmetrical dimethylarginine and mortality in patients with end-stage renal disease: a prospective study. *Lancet* 2001; **358**: 2113-2117.

40. Schmidt RJ, Yokota S, Tracy TS, et al. Nitric oxide production is low in end-stage renal disease patients on peritoneal dialysis. *Am J Physiol* 1999; **276**: F794-797.

41. Koyama H, Tabata T, Nishzawa Y, et al. Plasma endothelin levels in patients with uraemia. *Lancet* 1989; **1**: 991-992.

42. Annuk M, Zilmer M, Lind L, et al. Oxidative stress and endothelial function in chronic renal failure. *J Am Soc Nephrol* 2001; **12**: 2747-2752.

43. Amann K, Breitbach M, Ritz E, et al. Myocyte/capillary mismatch in the heart of uremic patients. *J Am Soc Nephrol* 1998; **9**: 1018-1022.

44. Levin A, Singer J, Thompson CR, et al. Prevalent left ventricular hypertrophy in the predialysis population: identifying opportunities for intervention. *Am J Kidney Dis* 1996; **27**: 347-354.

45. Levin A, Thompson CR, Ethier J, et al. Left ventricular mass index increase in early renal disease: impact of decline in hemoglobin. *Am J Kidney Dis* 1999; **34**: 125-134.

46. Foley RN, Parfrey PS, Harnett JD, et al. Clinical and echocardiographic disease in patients starting end-stage renal disease therapy. *Kidney Int* 1995; **47**: 186-192.

47. Silberberg JS, Barre PE, Prichard SS, et al. Impact of left ventricular hypertrophy on survival in end-stage renal disease. *Kidney Int* 1989; **36**: 286-290.

48. Haider AW, Larson MG, Benjamin EJ, et al. Increased left ventricular mass and hypertrophy are associated with increased risk for sudden death. *J Am Coll Cardiol* 1998; **32**: 1454-1459.

49. Wang MC, Tsai WC, Chen JY, et al. Arterial stiffness correlated with cardiac remodelling in patients with chronic kidney disease. *Nephrology (Carlton)* 2007; **12**: 591-597.

50. Chang KC, Tseng YZ, Kuo TS, et al. Impaired left ventricular relaxation and arterial stiffness in patients with essential hypertension. *Clin Sci (Lond)* 1994; **87**: 641-647.

51. Foley RN, Parfrey PS, Harnett JD, et al. The impact of anemia on cardiomyopathy, morbidity, and and mortality in end-stage renal disease. *Am J Kidney Dis* 1996; **28**: 53-61.

52. Harnett JD, Kent GM, Barre PE, et al. Risk factors for the development of left ventricular hypertrophy in a prospectively followed cohort of dialysis patients. *J Am Soc Nephrol* 1994; **4**: 1486-1490.

53. Parfrey PS, Foley RN, Harnett JD, et al. Outcome and risk factors for left ventricular disorders in chronic uraemia. *Nephrol Dial Transplant* 1996; **11**: 1277-1285.

54. Pannier B, Guerin AP, Marchais SJ, et al. Stiffness of capacitive and conduit arteries: prognostic significance for end-stage renal disease patients. *Hypertension* 2005; **45**: 592-596.

55. Blacher J, Guerin AP, Pannier B, et al. Impact of aortic stiffness on survival in end-stage renal disease. *Circulation* 1999; **99**: 2434-2439.

56. O'Rourke MF, Kelly RP. Wave reflection in the systemic circulation and its implications in ventricular function. *J Hypertens* 1993; **11**: 327-337.

57. London GM, Guerin AP, Marchais SJ, et al. Cardiac and arterial interactions in end-stage renal disease. *Kidney Int* 1996; **50**: 600-608.

58. Demuth K, Blacher J, Guerin AP, et al. Endothelin and cardiovascular remodelling in end-stage renal disease. *Nephrol Dial Transplant* 1998; **13**: 375-383.

59. Raggi P, Bellasi A, Ferramosca E, et al. Association of pulse wave velocity with vascular and valvular calcification in hemodialysis patients. *Kidney Int* 2007; **71**: 802-807.

60. Toussaint ND, Lau KK, Strauss BJ, et al. Associations between vascular calcification, arterial stiffness and bone mineral density in chronic kidney disease. *Nephrol Dial Transplant* 2008; **23**: 586-593.

61. London GM, Guerin AP, Marchais SJ, et al. Arterial media calcification in end-stage renal disease: impact on all-cause and cardiovascular mortality. *Nephrol Dial Transplant* 2003; **18**: 1731-1740.

62. Moe SM, O'Neill KD, Duan D, et al. Medial artery calcification in ESRD patients is associated with deposition of bone matrix proteins. *Kidney Int* 2002; **61**: 638-647.

63. Goodman WG, Goldin J, Kuizon BD, et al. Coronary-artery calcification in young adults with end-stage renal disease who are undergoing dialysis. *N Engl J Med* 2000; **342**: 1478-1483.

64. London GM, Marchais SJ, Guerin AP, et al. Arteriosclerosis, vascular calcifications and cardiovascular disease in uremia. *Curr Opin Nephrol Hypertens* 2005; **14**: 525-531.

65. Jono S, McKee MD, Murry CE, et al. Phosphate regulation of vascular smooth muscle cell calcification. *Circ Res* 2000; **87**: E10-17.

66. Reynolds JL, Joannides AJ, Skepper JN, et al. Human vascular smooth muscle cells undergo vesicle-mediated calcification in response to changes in extracellular calcium and phosphate concentrations: a potential mechanism for accelerated vascular calcification in ESRD. *J Am Soc Nephrol* 2004; **15**: 2857-2867.

67. Becker GJ, Hewitson TD. Animal models of chronic kidney disease: useful but not perfect. *Nephrol Dial Transplant* 2013; **28**: 2432-2438.

68. Hewitson TD, Ono T, Becker GJ. Small animal models of kidney disease: a review. *Methods Mol Biol* 2009; **466**: 41-57.

69. Wyngaarden JB, Dunn JT. 8-Hydroxyadenine as the intermediate in the oxidation of adenine to 2, 8-dihydroxyadenine by xanthine oxidase. *Arch Biochem Biophys* 1957; **70**: 150-156.

70. Peck CC, Bailey FJ, Moore GL. Enhanced solubility of 2,8 dihydroxyadenine (DOA) in human urine. *Transfusion* 1977; **17**: 383-390.

71. Shobeiri N, Adams MA, Holden RM. Vascular calcification in animal models of CKD: A review. *Am J Nephrol* 2010; **31**: 471-481.

72. Matsui I, Hamano T, Mikami S, et al. Fully phosphorylated fetuin-A forms a mineral complex in the serum of rats with adenine-induced renal failure. *Kidney Int* 2009; **75**: 915-928.

73. Henley C, Davis J, Miller G, et al. The calcimimetic AMG 641 abrogates parathyroid hyperplasia, bone and vascular calcification abnormalities in uremic rats. *Eur J Pharmacol* 2009; **616**: 306-313.

74. Lacour B, Lucas A, Auchere D, et al. Chronic renal failure is associated with increased tissue deposition of lanthanum after 28-day oral administration. *Kidney Int* 2005; **67**: 1062-1069.

75. Shobeiri N, Pang J, Adams MA, et al. Cardiovascular disease in an adenine-induced model of chronic kidney disease: the temporal link between vascular calcification and haemodynamic consequences. *J Hypertens* 2013; **31**: 160-168.

76. Levey AS. Measurement of renal function in chronic renal disease. *Kidney Int* 1990; **38**: 167-184.

77. Borsook H, Dubnoff JW. The hydrolysis of phosphocreatine and the origin of urinary creatinine. *J Biol Chem* 1947; **168**: 493-510.

78. Mulvany MJ, Halpern W. Contractile properties of small arterial resistance vessels in spontaneously hypertensive and normotensive rats. *Circ Res* 1977; **41**: 19-26.

79. Nilsson H, Sjoblom N. Distension-dependent changes in noradrenaline sensitivity in small arteries from the rat. *Acta Physiol Scand* 1985; **125**: 429-435.

80. Zoungas S, Asmar RP. Arterial stiffness and cardiovascular outcome. *Clin Exp Pharmacol Physiol* 2007; **34**: 647-651.

81. London GM, Guerin AP. Influence of arterial pulse and reflected waves on blood pressure and cardiac function. *Am Heart J* 1999; **138**: 220-224.

82. Cosson E, Herisse M, Laude D, et al. Aortic stiffness and pulse pressure amplification in Wistar-Kyoto and spontaneously

hypertensive rats. *Am J Physiol Heart Circ Physiol* 2007; **292**: H2506-2512.

83. Yokozawa T, Zheng PD, Oura H, et al. Animal model of adenine-induced chronic renal failure in rats. *Nephron* 1986; **44**: 230-234.

84. Ikeda R, Imai Y, Maruyama W, et al. Systemic disorders of calcium dynamics in rats with adenine-induced renal failure: implication for chronic kidney disease-related complications. *Nephrology (Carlton)* 2010; **15**: 54-62.

85. Katsumata K, Kusano K, Hirata M, et al. Sevelamer hydrochloride prevents ectopic calcification and renal osteodystrophy in chronic renal failure rats. *Kidney Int* 2003; **64**: 441-450.

86. Lomashvili KA, Monier-Faugere MC, Wang X, et al. Effect of bisphosphonates on vascular calcification and bone metabolism in experimental renal failure. *Kidney Int* 2009; **75**: 617-625.

87. Neven E, Dauwe S, De Broe ME, et al. Endochondral bone formation is involved in media calcification in rats and in men. *Kidney Int* 2007; **72**: 574-581.

88. Nagano N, Miyata S, Abe M, et al. Effect of manipulating serum phosphorus with phosphate binder on circulating PTH and FGF23 in renal failure rats. *Kidney Int* 2006; **69**: 531-537.

89. Johansson M, Gao SA, Friberg P, et al. Reduced baroreflex effectiveness index in hypertensive patients with chronic renal failure. *Am J Hypertens* 2005; **18**: 995-1000; discussion 1016.

90. Studinger P, Lenard Z, Mersich B, et al. Determinants of baroreflex function in juvenile end-stage renal disease. *Kidney Int* 2006; **69**: 2236-2242.

91. Saeed A, Dibona GF, Grimberg E, et al. High NaCl diet impairs dynamic renal blood flow autoregulation in rats with adenine-induced chronic renal failure. *Am J Physiol Regul Integr Comp Physiol* 2014.

92. Cowley AW, Jr. Long-term control of arterial blood pressure. *Physiol Rev* 1992; **72**: 231-300.

93. Johansson M, Gao SA, Friberg P, et al. Baroreflex effectiveness index and baroreflex sensitivity predict all-cause mortality and sudden death in hypertensive patients with chronic renal failure. *J Hypertens* 2007; **25**: 163-168.

94. Vallance P, Leone A, Calver A, et al. Accumulation of an endogenous inhibitor of nitric oxide synthesis in chronic renal failure. *Lancet* 1992; **339**: 572-575.

95. Closs EI, Basha FZ, Habermeier A, et al. Interference of L-arginine analogues with L-arginine transport mediated by the y+ carrier hCAT-2B. *Nitric Oxide* 1997; **1**: 65-73.

96. Nijveldt RJ, Van Leeuwen PA, Van Guldener C, et al. Net renal extraction of asymmetrical (ADMA) and symmetrical (SDMA) dimethylarginine in fasting humans. *Nephrol Dial Transplant* 2002; **17**: 1999-2002.

97. MacAllister RJ, Rambausek MH, Vallance P, et al. Concentration of dimethyl-L-arginine in the plasma of patients with end-stage renal failure. *Nephrol Dial Transplant* 1996; **11**: 2449-2452.

98. Schiffrin EL, Lipman ML, Mann JF. Chronic kidney disease: effects on the cardiovascular system. *Circulation* 2007; **116**: 85-97.

99. Arnal JF, Dinh-Xuan AT, Pueyo M, et al. Endothelium-derived nitric oxide and vascular physiology and pathology. *Cell Mol Life Sci* 1999; **55**: 1078-1087.

100. Arnal JF, Warin L, Michel JB. Determinants of aortic cyclic guanosine monophosphate in hypertension induced by chronic inhibition of nitric oxide synthase. *J Clin Invest* 1992; **90**: 647-652.

101. Ribeiro MO, Antunes E, de Nucci G, et al. Chronic inhibition of nitric oxide synthesis. A new model of arterial hypertension. *Hypertension* 1992; **20**: 298-303.

102. Navarro J, Sanchez A, Saiz J, et al. Hormonal, renal, and metabolic alterations during hypertension induced by chronic inhibition of NO in rats. *Am J Physiol* 1994; **267**: R1516-1521.

103. Fernandez-Rivas A, Garcia-Estan J, Vargas F. Effects of chronic increased salt intake on nitric oxide synthesis inhibition-induced hypertension. *J Hypertens* 1995; **13**: 123-128.

104. He FJ, Markandu ND, Sagnella GA, et al. Plasma sodium: ignored and underestimated. *Hypertension* 2005; **45**: 98-102.

105. Manunta P, Hamilton BP, Hamlyn JM. Salt intake and depletion increase circulating levels of endogenous ouabain in normal men. *Am J Physiol Regul Integr Comp Physiol* 2006; **290**: R553-559.

106. Manunta P, Messaggio E, Ballabeni C, et al. Plasma ouabain-like factor during acute and chronic changes in sodium balance in essential hypertension. *Hypertension* 2001; **38**: 198-203.

107. Manunta P, Rogowski AC, Hamilton BP, et al. Ouabain-induced hypertension in the rat: relationships among plasma and tissue ouabain and blood pressure. *J Hypertens* 1994; **12**: 549-560.

108. Manunta P, Stella P, Rivera R, et al. Left ventricular mass, stroke volume, and ouabain-like factor in essential hypertension. *Hypertension* 1999; **34**: 450-456.

109. Pierdomenico SD, Bucci A, Manunta P, et al. Endogenous ouabain and hemodynamic and left ventricular geometric patterns in essential hypertension. *Am J Hypertens* 2001; **14**: 44-50.

110. Rossi G, Manunta P, Hamlyn JM, et al. Immunoreactive endogenous ouabain in primary aldosteronism and essential hypertension: relationship with plasma renin, aldosterone and blood pressure levels. *J Hypertens* 1995; **13**: 1181-1191.

111. Wilkinson IB, MacCallum H, Hupperetz PC, et al. Changes in the derived central pressure waveform and pulse pressure in response to angiotensin II and noradrenaline in man. *J Physiol* 2001; **530**: 541-550.

112. Mulvany MJ, Aalkjaer C, Christensen J. Changes in noradrenaline sensitivity and morphology of arterial resistance vessels during development of high blood pressure in spontaneously hypertensive rats. *Hypertension* 1980; **2**: 664-671.

113. Koobi P, Kalliovalkama J, Jolma P, et al. AT1 receptor blockade improves vasorelaxation in experimental renal failure. *Hypertension* 2003; **41**: 1364-1371.

114. Vettoretti S, Ochodnicky P, Buikema H, et al. Altered myogenic constriction and endothelium-derived hyperpolarizing factor-mediated relaxation in small mesenteric arteries of hypertensive subtotally nephrectomized rats. *J Hypertens* 2006; **24**: 2215-2223.

115. New DI, Chesser AM, Thuraisingham RC, et al. Structural remodeling of resistance arteries in uremic hypertension. *Kidney Int* 2004; **65**: 1818-1825.

116. Hasdan G, Benchetrit S, Rashid G, et al. Endothelial dysfunction and hypertension in 5/6 nephrectomized rats are mediated by vascular superoxide. *Kidney Int* 2002; **61**: 586-590.

117. Wu-Wong JR, Noonan W, Nakane M, et al. Vitamin d receptor activation mitigates the impact of uremia on endothelial function in the 5/6 nephrectomized rats. *Int J Endocrinol* 2010; **2010**: 625852.

118. Griffin KA, Picken MM, Churchill M, et al. Functional and structural correlates of glomerulosclerosis after renal mass reduction in the rat. *J Am Soc Nephrol* 2000; **11**: 497-506.

119. Ibrahim HN, Hostetter TH. The renin-aldosterone axis in two models of reduced renal mass in the rat. *J Am Soc Nephrol* 1998; **9**: 72-76.

120. Loot AE, Schreiber JG, Fisslthaler B, et al. Angiotensin II impairs endothelial function via tyrosine phosphorylation of the endothelial nitric oxide synthase. *J Exp Med* 2009; **206**: 2889-2896.

121. Bragulat E, Larrousse M, Coca A, et al. Effect of long-term irbesartan treatment on endothelium-dependent vasodilation in essential hypertensive patients. *Br J Biomed Sci* 2003; **60**: 191-196.

122. Malik RA, Schofield IJ, Izzard A, et al. Effects of angiotensin type-1 receptor antagonism on small artery function in patients with type 2 diabetes mellitus. *Hypertension* 2005; **45**: 264-269.

123. Wassmann S, Hilgers S, Laufs U, et al. Angiotensin II type 1 receptor antagonism improves hypercholesterolemia-associated endothelial dysfunction. *Arterioscler Thromb Vasc Biol* 2002; **22**: 1208-1212.

124. Sutliff RL, Walp ER, El-Ali AM, et al. Effect of medial calcification on vascular function in uremia. *Am J Physiol Renal Physiol* 2011; **301**: F78-83.

125. Diwan V, Mistry A, Gobe G, et al. Adenine-induced chronic kidney and cardiovascular damage in rats. *J Pharmacol Toxicol Methods* 2013; **68**: 197-207.

126. Amann K, Wolf B, Nichols C, et al. Aortic changes in experimental renal failure: hyperplasia or hypertrophy of smooth muscle cells? *Hypertension* 1997; **29**: 770-775.

127. Fakhouri F, Placier S, Ardaillou R, et al. Angiotensin II activates collagen type I gene in the renal cortex and aorta of transgenic mice through interaction with endothelin and TGF-beta. *J Am Soc Nephrol* 2001; **12**: 2701-2710.

128. Ohama T, Hori M, Fujisawa M, et al. Downregulation of CPI-17 contributes to dysfunctional motility in chronic intestinal inflammation model mice and ulcerative colitis patients. *J Gastroenterol* 2008; **43**: 858-865.

129. Su W, Xie Z, Liu S, et al. Smooth muscle-selective CPI-17 expression increases vascular smooth muscle contraction and blood pressure. *Am J Physiol Heart Circ Physiol* 2013; **305**: H104-113.

130. Deng HW, Kwan CY. Cyclopiazonic acid is a sarcoplasmic reticulum Ca(2+)-pump inhibitor of rat aortic muscle. *Zhongguo Yao Li Xue Bao* 1991; **12**: 53-58.

131. Luik RM, Wu MM, Buchanan J, et al. The elementary unit of store-operated Ca2+ entry: local activation of CRAC channels by STIM1 at ER-plasma membrane junctions. *J Cell Biol* 2006; **174**: 815-825.

132. Mancarella S, Potireddy S, Wang Y, et al. Targeted STIM deletion impairs calcium homeostasis, NFAT activation, and growth of smooth muscle. *FASEB J* 2013; **27**: 893-906.

133. Freichel M, Suh SH, Pfeifer A, et al. Lack of an endothelial store-operated Ca2+ current impairs agonist-dependent vasorelaxation in TRP4-/- mice. *Nat Cell Biol* 2001; **3**: 121-127.

134. Tiruppathi C, Freichel M, Vogel SM, et al. Impairment of store-operated Ca2+ entry in TRPC4(-/-) mice interferes with increase in lung microvascular permeability. *Circ Res* 2002; **91**: 70-76.

135. Moore ED, Etter EF, Philipson KD, et al. Coupling of the Na+/Ca2+ exchanger, Na+/K+ pump and sarcoplasmic reticulum in smooth muscle. *Nature* 1993; **365**: 657-660.

136. Pritchard TJ, Bowman PS, Jefferson A, et al. Na(+)-K(+)-ATPase and Ca(2+) clearance proteins in smooth muscle: a functional unit. *Am J Physiol Heart Circ Physiol* 2010; **299**: H548-556.

137. Simchon S, Manger W, Golanov E, et al. Handling 22NaCl by the blood-brain barrier and kidney: its relevance to salt-induced hypertension in dahl rats. *Hypertension* 1999; **33**: 517-523.

138. Nakamura K, Cowley AW, Jr. Sequential changes of cerebrospinal fluid sodium during the development of hypertension in Dahl rats. *Hypertension* 1989; **13**: 243-249.

139. Wang H, Huang BS, Leenen FH. Brain sodium channels and ouabainlike compounds mediate central aldosterone-induced hypertension. *Am J Physiol Heart Circ Physiol* 2003; **285**: H2516-2523.

140. Zhang ZH, Yu Y, Kang YM, et al. Aldosterone acts centrally to increase brain renin-angiotensin system activity and oxidative stress in normal rats. *Am J Physiol Heart Circ Physiol* 2008; **294**: H1067-1074.

141. Huang BS, White RA, Ahmad M, et al. Central infusion of aldosterone synthase inhibitor attenuates left ventricular dysfunction and remodelling in rats after myocardial infarction. *Cardiovasc Res* 2009; **81**: 574-581.